Wennekes Lab
Chemical Glycobiology

Utrecht University

UIPS Utrecht Institute for Pharmaceutical Sciences

Utrecht Institute for Pharmaceutical Sciences
Bijvoet Center for Biomolecular Research
Chemical Biology and Drug Discovery – Wennekes Lab

Attempts at the synthesis of a novel sialic acid ABPP probe for viral neuraminidases

Minor Internship Report 2023
Jochem de Waard
9669035

Molecular and Cellular Life Sciences (MSc)

Examiner:	Dr. Tom Wennekes
Daily supervisor:	Lemeng Chao, MSc
Second reviewer:	Prof. Dr. Roland Pieters

Utrecht, November 2023

Table of contents

1 Abstract

The influenza virus causes a common acute respiratory infection, affecting around 1 billion humans annually and resulting in 290-650 thousand respiratory deaths yearly. The viruses use glycoproteins hemagglutinin and neuraminidase to enter and spread throughout cells of the host. Targeting the neuraminidases with activity-based protein profiling (ABPP) can give us great insight into the virus's workings. ABPP uses chemical probes to specifically label active enzymes of interest. Incorporation of a recognition element in the ABPP achieves specificity, which drives the probe to the target. For viral neuraminidases substrate sialic acid, a nine-carbon monosaccharide often found on the terminus of glycoconjugates and highly important for the entry and spread of the viral particles, is an appropriate recognition element. Incorporating a reactive group that covalently binds the target allows for stable and long-lasting binding of the probe. Installing a difluoro motif on the sialic acid causes the covalently bound intermediate to be trapped in the active site of viral neuraminidases. Finally, the probe contains a clickable tag that acts as a latent reporter element. Although ABPP probes for difluoro sialic acid have been developed, they feature a clickable element that compromises crucial interactions within the neuraminidases' active site. Consequently, our emphasis in this study is on incorporating the clickable tag at the C7 position of sialic acid, which has no interactions within the neuraminidase active site.

N-acetylated sialic acid was first modified to accept the difluoro motif by installing a double bond between the C2 and C3 positions. Simultaneously, an azide was installed on the C4 position and converted into a Boc protected amine. Next, the C8 and C9 positions were selectively protected by an isopropylidene acetal. Installing an azide directly on the C7 position, either via a Mitsunobu conversion or an S_N2 nucleophilic substitution proved highly difficult. Therefore, installing a small spacer molecule onto the C7 position with a terminal azide was attempted. However, both an ether-bond linker and a carbamate linker could not be successfully installed. A C7-azide neuraminidase ABPP probe could not be successfully synthesized. Alternative approaches of obtaining the C7-azide clickable ABPP probe were theorized. For instance, further optimization of the spacer attachment reactions or applying a chemoenzymatic approach.

2 Layman summary

An influenza infection, caused by the influenza virus, is not usually dangerous towards healthy individuals. However, younger, older or patients with a weakened immune system can be at serious risk when infected with the influenza virus. The currently available drugs prevent the spread of the virus throughout the host by inhibiting an enzyme that is highly important in the viruses life cycle. Nevertheless, as resistance to these drugs is on the rise, the scientific community is redirecting its efforts towards designing anti-influenza drugs that inhibit the virus in a manner that makes it challenging to develop resistance. To achieve this, the natural substrate of this important enzyme was modified so that it stays covalently bound within the enzyme, preventing the virus from being able to spreading further.

These newly designed drugs can be further modified to help us better understand the viruses workings, and its enzymes that help it spread through the infected host, using activity based protein profiling (ABPP). The primary goal of ABPP is to identify and understand the functions of active enzymes in a biological setting. This goal is achieved by designing chemical probes that mimic the natural substrate of the enzymes they act upon. The chemical probes consist of three distinct components: recognition, reactive, and reporter elements. The recognition element is used to drive the probe towards its intended target, while the reactive element guarantees long-lasting, covalent, binding with the target. The newly designed inhibitors already contain these two elements specific towards the influenza virus and its enzymes. Therefore, the goal of this research is to add the third and final important element for an ABPP probe: a reporter element. This can be used to visualize the virus and its enzymes, for instance in its native environment, or to purify it from a complex mixture. In prior research a working ABPP probe for an influenza enzyme, however, the reporter element was put on a position that would likely reduce binding efficiency with the target. Moreover, selectivity towards viral neuraminidases was not optimized. Therefore, within this research it was attempted to install on a novel position that is known to not have any interactions, likely not perturbing binding efficiency, while also improving the selectivity towards viral neuraminidases.

The natural substrate of the neuraminidase enzyme, sialic acid, was taken as the starting point of the whole synthesis, since this is a good recognition element. This was first modified so that it can accept the installation of the important reactive groups. Selectivity improving groups were introduced on the recognition element of the probe to create specificity for viral enzymes. Finally, it was attempted to install the reporter tag on the novel position. However, this proved to be more difficult than initially anticipated. An explanation for why modification of this specific position was not achieved could be the highly unreactive nature of this position. Together with potential impurities that could not be removed, or even identified. Thus, a novel ABPP probe for the neuraminidase enzyme was not successfully synthesized. Different approaches for obtaining the novel ABPP probe were theorized. For instance, utilizing the enzymes responsible for synthesizing sialic acid within cells and supplying them modified starting materials, leading to the formation of the desired neuraminidase ABPP probe.

3 Introduction

3.1 Sialic acid and the influenza virus

Sialic acid, or neuraminic acid (Neu), a monosaccharide with a nine carbon backbone, is often found at the terminal position of glycoconjugates. When considering the different isomers of sialic acid, they are prevalent in virtually all vertebrates. In humans the most common sialic acid is the *N*-acetylated form (Neu5Ac), while in many other animals the *N*-glycolylated forms are more abundant (Neu5Gc) (Figure 1A) [1].

The large family of sialic acids is still growing and currently consists of more than 50 derivatives [1, 2]. Multiple *O*-substitutions can take place on the C4, -7, -8 and -9 positions, as well as the formation of a double bond between C2 and -3, giving rise to a plethora of possible isomers. The large structural diversity highlights the importance of this sugar in many different biological processes [3]. Important functions of sialic acids are cell-cell recognition, aggregation, development, carbohydrate-protein interactions, controlling lifetimes of glycoconjugates, tumour growth and metastasis [2]. Arguably the most important process is forming the receptor or ligands in cell-cell communication, and thus many host-pathogen interactions have evolved that abuse sialic acid, due to their preferred placement at the terminus of glycoconjugates [4].

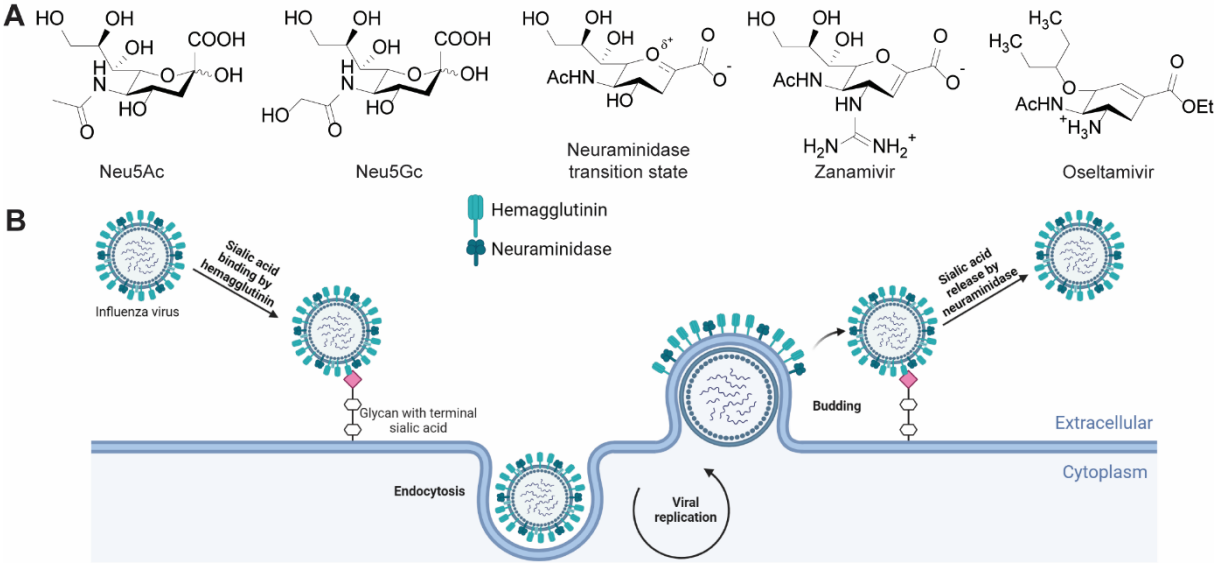

Figure 1 A) Chemical structures of N-acetylated sialic acid (Neu5Ac), N-glycolylated sialic acid (Neu5Gc), transition state sialic acid in neuraminidases and established anti-influenza drugs zanamivir (Relenza) and oseltamivir (Tamiflu), respectively. B) Schematic representation of the cellular entry and leaving mechanism employed by influenza viruses.

Influenza is a common acute respiratory infection that is especially dangerous for young children, immunocompromised individuals and adults aged 65 years and older. The WHO estimates 1 billion human influenza cases each year, of which approximately 3 to 5 million cases are classified as a severe illness. Moreover, about 290.000 to 650.000 respiratory deaths occur annually because of an influenza infection, highlighting the significant impact of influenza on society [5, 6]. The influenza virus attaches to, and removes, cellular sialic acids as part of their entry and spreading mechanisms [7]. These viruses possess hemagglutinins (HA) and neuraminidases (NA) on their cellular envelope. These glycoproteins, or sialidases, are used by the pathogens to invade the host and are essential in viral infections and the spread thereof [4, 8]. HA can recognize and bind sialic acids located on the terminus of glycoconjugates, thereby initiating cellular entry. In the cell, the virus is able to replicate and upon completion NA can cleave the sialic acid from the viral- and cellular surface, allowing the virus to spread [8] (Figure 1B). Inhibition of these viral sialidases has already been achieved by known anti-influenza drugs; zanamivir

(Relenza) and oseltamivir (Tamiflu) (Figure 1A). These drugs inhibit NA, in a reversible manner, by mimicking the transition state of sialic acid in the binding pocket of the sialidase (Figure 1A). However, resistance against these reversible drugs is emerging. Resistance is especially dangerous for individuals that have a high risk of developing a severe illness from an influenza infection, such as young children, immunocompromised patients and the elderly [6]. An alternative way to inactivate NA, and potentially new type of influenza drug, is via mechanism-based NA inactivation, which bind covalently to the active site of viral NA [8]. The structural modifications of sialic acid used in these drugs can be of high interest in developing sialidase activity-based protein profiling probes. These probes can be used to achieve a greater understanding of sialidase activity.

3.2 Sialidase activity-based protein profiling

Using activity-based protein profiling (ABPP) to gain an increased understanding of sialidase activity in sialic acid-dependant pathological pathways can be of great benefit. ABPP uses chemical probes to specifically label a target enzyme of interest. This is achieved by designing and chemically synthesizing a molecule, the chemical probe, that mimics the substrate, but hijacks the catalytic mechanism of the target enzyme to covalently inactivate it via a reactive group. Another component of the probe contains a tag that is used as either a reporter or an affinity label. The ABPP probe for sialidases should contain recognition element which resemble sialic acid closely, a reactive group which ensures covalent binding, and a reporter tag which can be modified accordingly.

Covalent binding is a requisite for an ABPP probe since this is more specific and increases binding longevity. NAs accommodate a specific binding pocket for sialic acids and a specific residue of influenza sialidases, Y406, performs a nucleophilic attack on the C2 position to form a covalently bound intermediate with sialic acid (Figure 2A/B). Established chemical modifications of sialic acid derivatives that increase the rate constant for intermediate formation and decrease the rate constant for hydrolysis to trap the intermediate will ensure a longstanding bond. Introducing a fluorine on the C3 position of sialic acid has been known to significantly reduce the rate of hydrolysis of sialic acid from residue Y406 in sialidases. This is due to the strong electron-withdrawing effect of fluorine, which destabilizes the transition state. Destabilization of the transition state makes hydrolysis of the covalent bond energetically unfavourable. Introduction of a fluorine in the C2 position speeds up the formation of the bond between the sialidase and sialic acid by being a good leaving group. Both chemical modifications cause the intermediate to be trapped and thus facilitate an effective reactive group for a ABPP probe for sialidases (Figure 2A/B) [8].

The tag group of the ABPP probe for sialidases that is investigated within this work is an azide group. Azides can undergo a Cu(I)-catalyzed azide-alkyne [3+2] cycloaddition (CuAAC), when introduced to a terminal alkyne moiety. The CuAAC reaction is an example of a click-reaction, a type of reaction which joins two small units together with high efficiency, stereospecificity and good yields [9]. These qualities make an azide a good taggable moiety for a ABPP probe.

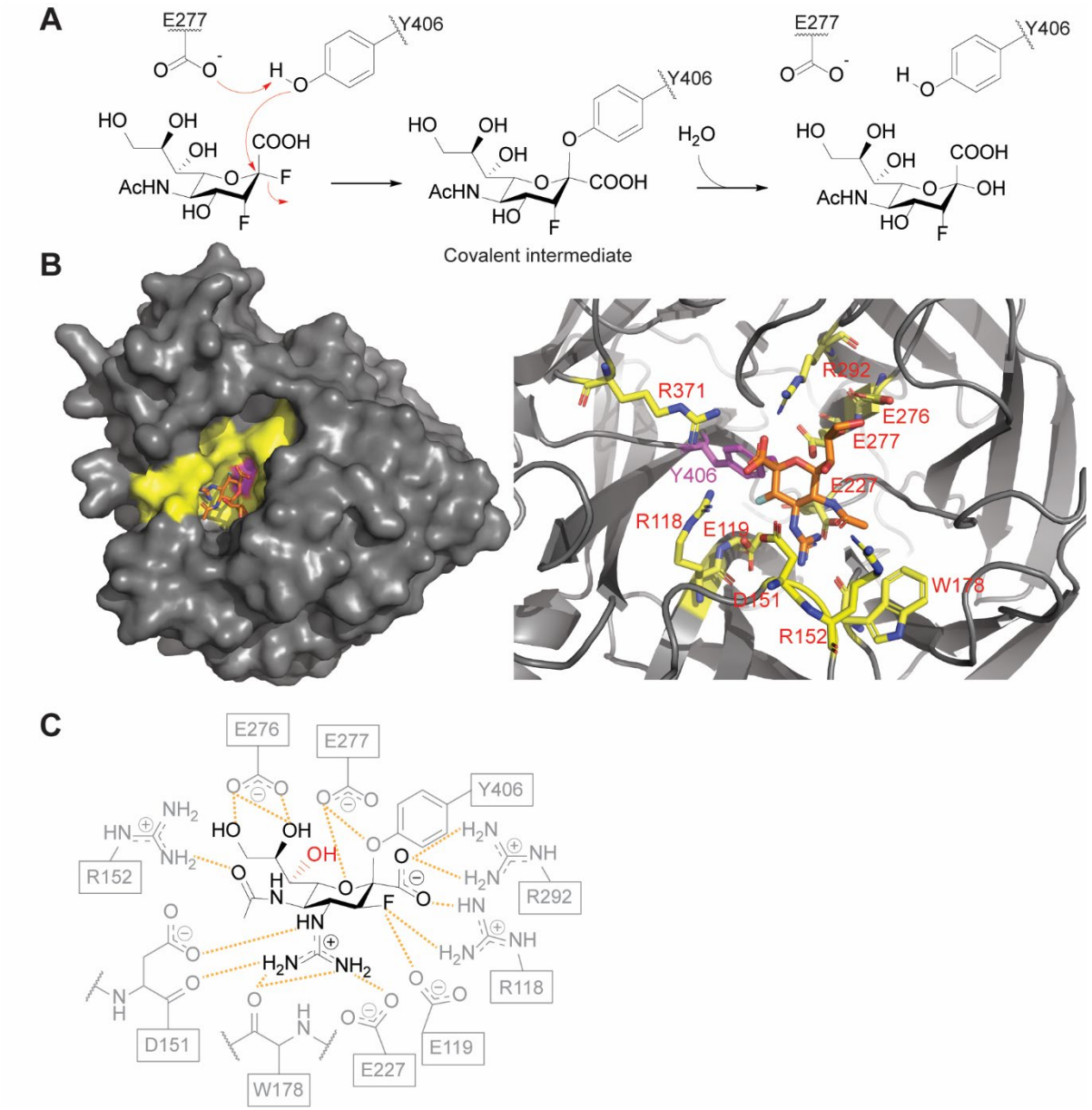

Figure 2 A) Binding mechanism for sialic acid and the effects of known fluorine modifications. B) Neuraminidase surface model with C3-F sialic acid trapped (orange) in its active site (highlighted yellow). The residue, Y406, that forms a covalent bond is highlighted in purple (left). Zoom in on neuraminidases active site trapped with C3-F sialic acid (orange). The residues that have interactions are coloured in yellow and the residue, Y406, that forms a covalent bond is highlighted in purple (right). C) Schematic representation of the hydrogen bonding patterns between 3-fluoro-4-guanidino sialic acid and influenza NA, as determined by the Withers group (2013) [8] using X-ray crystallography. The C7 hydroxyl without interactions is highlighted in red. (Figures adapted from: [8])

ABPP sialidase probes containing a fluorine in the C2 and C3 position of sialic acid have already been realized. Tsai et al. (2013) created a cell-permeable probe which was able to label viral, bacterial and human sialidases. Their probe contained the taggable alkyne moiety on the C5 position of sialic acid [10]. The Withers group (2013) used X-ray crystallography to reveal the hydrogen bonding patterns of 3-fluoro-4-guanidino-sialic acid trapped in influenza NA (Figure 2C). This identified an important hydrogen bond between the acetyl group on position C5 with residue R152 of influenza NA [8]. The taggable moiety on the Tsai et al. (2013) probe results in a lost interaction, likely reducing the binding affinity between probe and enzyme. Moreover, their probe did not contain any moieties to increase the specificity towards viral NAs, making unwanted labelling of non-viral NAs more likely. The X-ray crystallography structure reveals that C7 hydroxyl points into the solvent without any interactions (Figure 2C). Within this work an attempt was made to synthesize 2,3-difluoro-sialic acid with an taggable moiety on the C7 position. A taggable moiety at this position of sialic acid could be beneficial for the binding affinity of the probe to the target, since this does not perturb any important hydrogen bonds. Moreover, since the C7 hydroxyl aims towards the solvent, a larger moiety on this position likely would not be perturbed by interactions or steric hinderance with the rest of the NA. Therefore, a taggable moiety could have more space on the C7 position compared to other positions. Finally, to increase the selectivity towards viral NAs an amine was installed on the C4 position [8].

3.3 Synthesis plan of novel sialidase ABPP probe

The research described in this work investigates multiple synthetic routes for creating a novel ABPP probe for viral sialidases that contains a clickable azide moiety on the C7 position of sialic acid. The initially designed synthesis route starts with preparing *N*-acetylated sialic acid for accepting the difluoro motif and installing an azide on the C4 position. Next, the C8 and C9 position are selectively protected and the C4 azide converted into a protected amine. With only the C7 hydroxyl remaining unprotected various pathways of installing an azide on this position are investigated. The initial goal was to install the clickable tag directly on the C7 position. Besides that, pathways that utilize a small spacer molecule are also investigated. Finally, the difluoro motif would be installed and protecting group removal would produce the final probes (scheme 1).

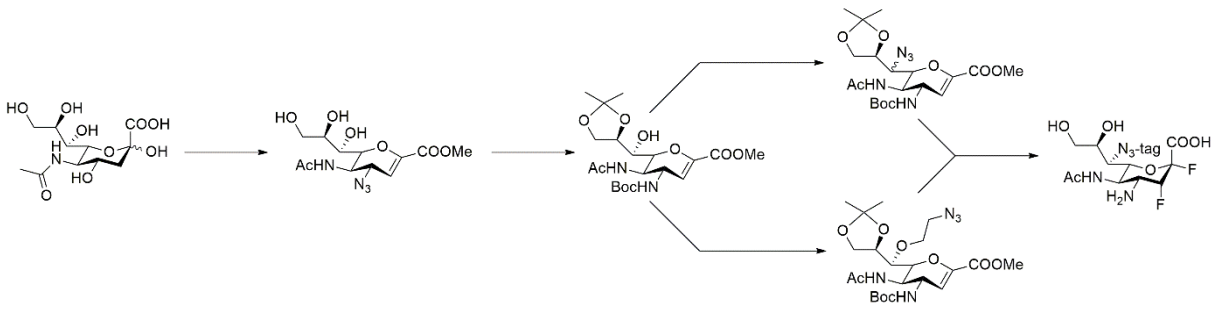

Scheme 1) The initially proposed synthesis route for creating a C7-N_3-difluoro sialic acid ABPP probe for viral sialidases. Starting from N-acetylated sialic acid, which would first be prepared to accept the difluoro motif. Next, the C8 and C9 position would be selectively protected, while the C4 azide would be converted into a protected amine. Thereafter, multiple pathways for installing an azide on the C7 position would be researched. Finally, the difluoro motif would be installed and the protection groups removed.

With the ABPP probe completed, the next steps would be to click a biotin or a fluorescent reporter onto the azide, via CuAAC, to identify the labelled sialidases. Finally, the probe would tested by incubating it with sialidase monomers, dimers and tetramers to investigate whether labelling would be achieved.

4 Results and discussion

A novel ABPP probe that selectively targets sialidases could be highly valuable in enhancing our comprehension of sialidase activity. ABPP probes consist of a recognition element, the component that closely resembles sialic acid, a reactive group that ensures long binding, and a tag that can be used as a reporter or affinity label. CuAAC click chemistry was chosen for the taggable element of the probe, since this is efficient, stereospecific and results in good yields.

4.1 Preparation of per-*O*-acetylated, C4 azide sialic acid glycal

Before the taggable element can be installed, sialic acid was adapted to accept the difluoro motif and the other functional groups of sialic acid were protected. Previously established protocols were used for these reactions [11, 12]. Neu5Ac was used as an initial starting point (Figure 1A). The carboxylic acid at the C1 position underwent Fischer esterification in methanol which resulted in protection by a methyl ester. Next, the remaining free hydroxyls were acetylated by having acetic anhydride react in the presence of pyridine. With all the functional groups protected a 5-membered ring was installed on C4 and C5 and a double bond was installed between C2 and C3 by adding trimethylsilyl trifluoromethanesulfonate (TMSOTf). The TMS acts as a good leaving group for the instalment of the triflate group. The triflate group simultaneously activated the C4- and the C2 hydroxyls. Next, the C5 acetyl group and C3 hydrogen performed intermolecular attacks on the activated hydroxyls to give rise to a 5-membered ring on the C4 and C5 position and a double bond between C2 and C3 positions of sialic acid, respectively. The 5-membered ring activated the C4 position for azide introduction. Azides can easily be converted into amines via reduction; an amine on the C4 position of sialic acid increases the selectivity towards viral neuraminidases [8]. Azidotrimethylsilane ($TMSN_3$) provides a nucleophilic azide that attacks the C4 position, breaking the 5-membered ring which resulted in the primed sialic acid glycal (Scheme 2). All reactions were performed according to the literature and resulted in the expected yields.

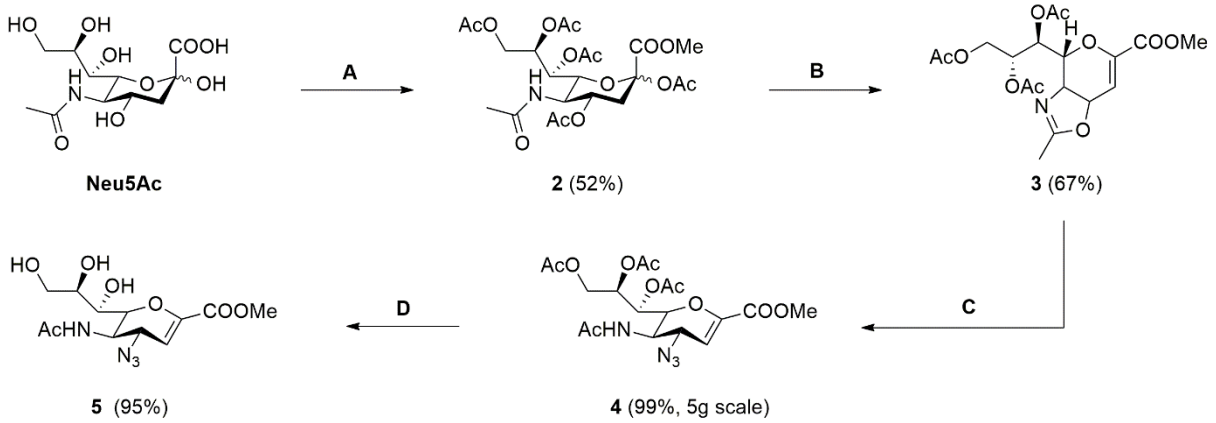

Scheme 2) Synthesis of per-O-acetylated-C4-azido-sialic acid glycal and its O-acetyl deprotection. Conditions: A) H+, MeOH, RT, o/n. B) Ac_2O, Pyridine, RT, o/n. C) i) TMSOTf, EtOAc, 50°C, 3h. D) $TMSN_3$, Tert-butanol, 80°C, o/n. E) Sodium methoxide, MeOH, H+, RT, 3h.

4.2 Installing the clickable tag before the difluoro motif

With the glycal synthesis completed the C7 hydroxyl was deprotected in order to install a taggable moiety. Therefore, the *O*-acetyls were deprotected using sodium methoxide (MeONa) in methanol. To prevent hydrolysis of the methyl ester, the reaction was performed under water-free conditions. Sodium methoxide was quenched by the addition of amberlite H120 (Scheme 2). The C8 and C9 positions were initially protected as a benzylidene acetal using (dimethoxymethyl)-benzene. However, this resulted in a 1:1 mixture of endo- and exo-isomers of the benzylidene acetal with respect to the 5-membered ring that establishes. The different isomers established because rotation is not possible around C10 position (Figure 3A). Both isomers could be used in the coming reactions, however, this would further complicate the thin layer chromatography (TLC) analysis of reactions and therefore a better alternative was investigated. Using 2,2-dimethoxypropane resulted in the protection of C8 and C9, while the endo- and exo-isomers were identical, which ensured an easier TLC readout (Scheme 3).

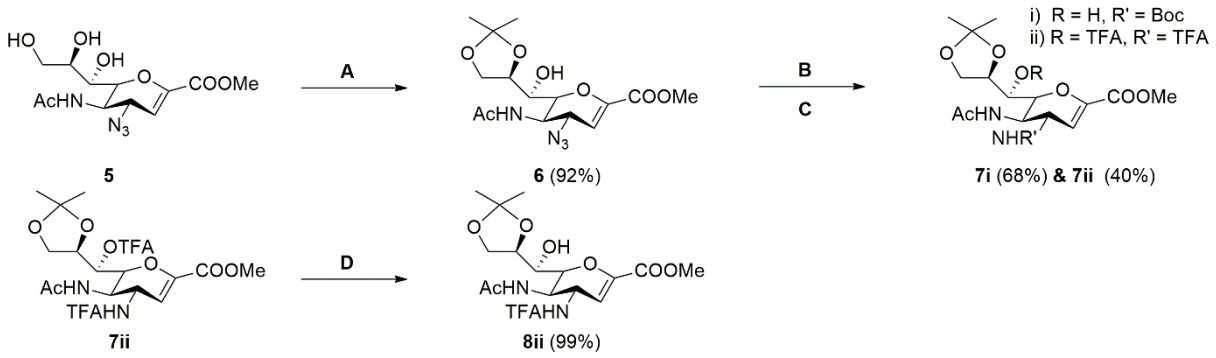

Scheme 3) Synthesis of free C7 hydroxyl and converting azide into a protected amine. Conditions: A) 2,2-dimethoxy propane, camphor sulfonic acid, acetonitrile, 0°C-RT, 2h. B) Triphenylphosphine ($P(Ph)_3$), Di-tert-butyl dicarbonate, $NaHCO_3$, THF:H_2O (5:1), 60°C-RT, o/n. C) $P(Ph)_3$, THF/H_2O (5:1), 60°C, o/n, trifluoromethanesulfonic anhydride, triethylamine, THF, 0°-RT, 2h. D) K_2CO_3, MeOH, RT, 2h.

The clickable tag for the C7 position was chosen to be an azide. This was chosen because an alkyne would be incompatible during the instalment of the difluoro motif. However, this also meant that the C4 azide had to be converted into a protected amine, prior to installing the clickable tag. First, the azide was reduced by a Staudinger reduction using triphenylphosphine ($P(Ph)_3$). A Staudinger reduction was chosen to ensure that only the azide was reduced and not the double bond on the C2 and C3 positions, which would happen under hydrogen reduction conditions. Next, two different amine protection groups were tried. Initially installing a trifluoroacetamide was tested, by having the amine react with trifluoroacetic anhydride in the presence of triethylamine. These conditions resulted in a trifluoroacetamide group on both the C4 amine and C7 hydroxyl, proven by the ^{19}Fluorine nuclear magnetic resonance (NMR) spectrum displaying two peaks (Figure 3B). The trifluoroacetamide group on the C7 hydroxyl was removed with a mild base, however, with enough time this would also hydrolyse the C4 trifluoroacetamide protection, further complicating the reaction (Figure 3B). An attempt to mitigate the protection of the C7 hydroxyl using the less reactive ethyl trifluoroacetate was performed, however this resulted in no conversion (Scheme 3).

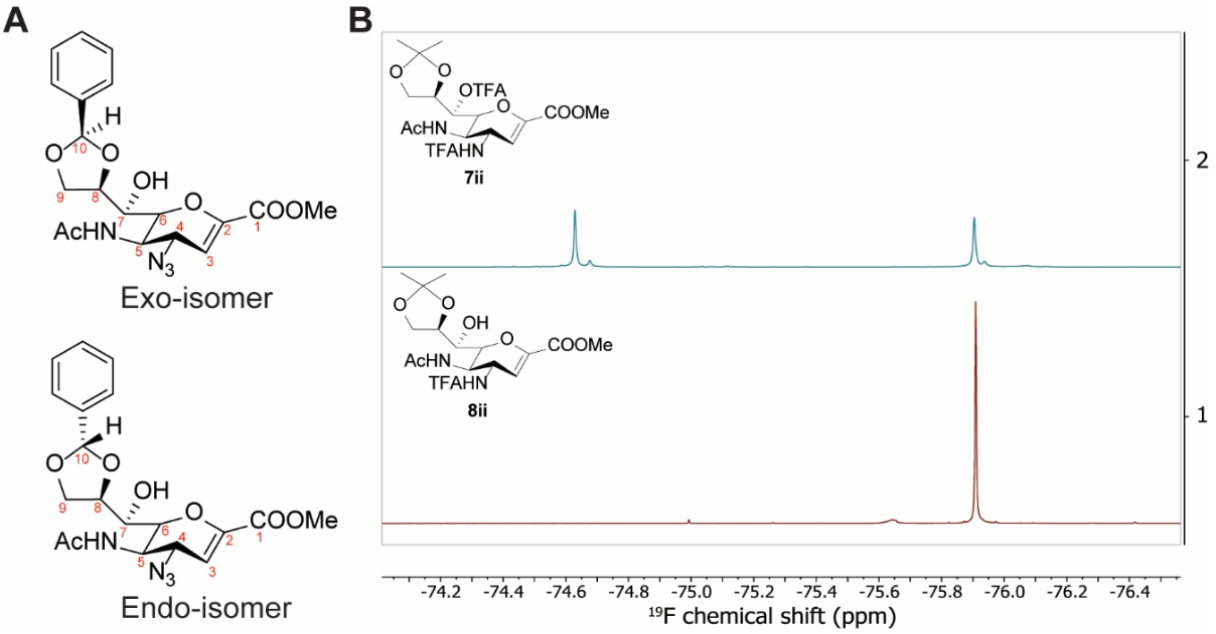

Figure 3 A) Exo- and endo-isomer schematic structures highlighting the inability to rotate around the C10 position. B) Stacked ^{19}fluorine NMR spectra of (7ii), proving the attachment of a TFA protection group on both C4 amine and C7 hydroxyl (top panel, 2), and (8ii), proving the removal of the C7 hydroxyl TFA group (bottom panel, 2).

As a consequence of the complicated reaction, installing a tert-butyloxycarbonyl (Boc) protection group was investigated. A one-pot solution was applied. First the Staudinger reduction with $P(Ph)_3$ was deployed until completion, as indicated by TLC. Next, the mixture was cooled to room temperature followed by addition of di-tert-butyl dicarbonate and sodium bicarbonate to install the Boc group on the free amine. The free amine performs a nucleophilic attack on the carbonyl in di-tert-butyl dicarbonate. The base deprotonates the amine in the intermediate, speeding up the reaction. This resulted in a reproducible reaction with respectable yields (60-70%) and a pure product, as indicated by proton NMR (Scheme 3).

4.3 Installing an azide directly on the C7 hydroxyl

With all the functional groups protected, except for the C7 hydroxyl, instalment of the clickable tag was investigated. Initially, direct conversion of the C7 hydroxyl to an azide was attempted. A Mitsunobu hydroxyl to azide substitution was attempted first. During this substitution diisopropyl azodicarboxylate (DIAD) was activated by having $P(Ph)_3$ perform a nucleophilic attack generating a phosphonium intermediate. The intermediate binds to the hydroxyl oxygen, activating the leaving group. Next, diphenylphosphoryl azide (DPPA) provides an azide as a nucleophile which can attack on the hydroxyl position, cleanly inverting the stereochemistry. The inverted stereochemistry would not be doubly inverted for testing purposes.

The Mitsunobu substitution was tried two times (Scheme 4). Commonly reactions are left overnight, however, even when the reaction was left for 48 hours no conversion was seen. Firstly, the quality of the reagents DPPA and DIAD were measured with NMR, which revealed the expected peaks (Figure S1A/B, respectively). Moreover, water interferes with the reactivity of the reagents, thus freshly dried THF (using activated 4Å molsieves) was used the second time. Again, no conversion was seen, therefore it was determined that the hydroxyl was not reactive enough to undergo Mitsunobu conversion. Another possible explanation for the observed unreactive nature could be that the C7 hydroxyl is too sterically hindered for the relatively large reagents used during the Mitsunobu conversion.

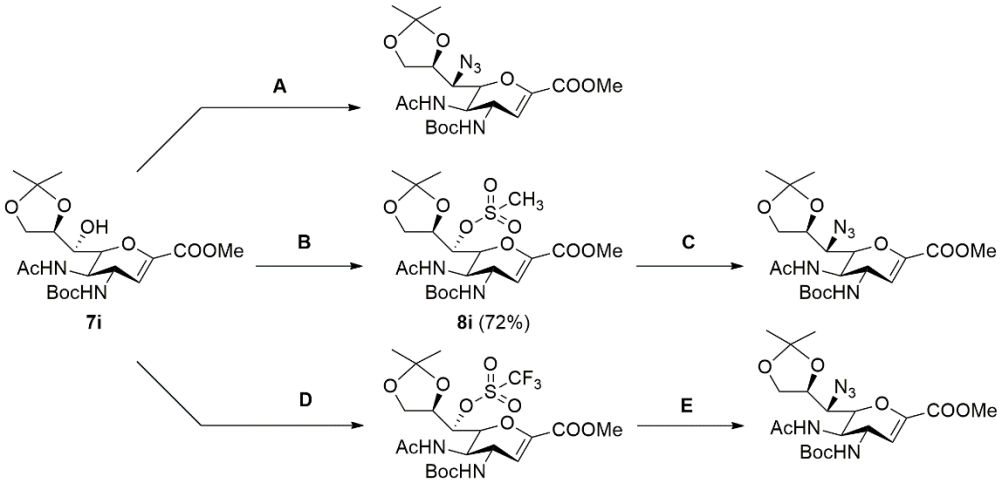

Scheme 4) Different synthesis routes investigated for installing an azide tag directly on the C7 position of sialic acid. Conditions: A) Diisopropyl azodicarboxylate (DIAD), Diphenylphosphoryl Azide (DPPA), $P(Ph)_3$, THF, 0°C-RT, o/n. B) Methanesulfonyl chloride, triethylamine, DMAP, DCM, RT, 48h. C) Sodium azide, Tetrabutylammonium azide, DMF, 80°C, o/n. D) Trifluoromethanesulfonic anhydride, 2,6-Lutidine/Pyridine, DCM, -78°C/-10°C, 2h/o/n. E) Tetrabutylammonium azide, DCM/toluene, -78°C-RT/70-110°C, 2h.

After the failed Mitsunobu substitution, activation of the C7 hydroxyl was tried by converting it to a better leaving group. Initially, a methanesulfonyl group was successfully installed on the C7 hydroxyl, by having it react with methanesulfonyl chloride (MsCl) in the presence of triethylamine (Scheme 4). The free hydroxyl performed a nucleophilic attack on the sulphur and the chlorine was kicked from the MsCl. The triethylamine acted as a base by deprotonating the hydroxyl, speeding up the reaction. The success of the reaction was determined by proton NMR, which revealed a CH_3 peak in the expected chemical shift region. The methanesulfonyl group should be a better leaving group, since it is a much weaker base and has the possibility to form resonance structures. However, when a nucleophilic azide was introduced to have it perform a S_N2 nucleophilic substitution, no conversion was seen. To increase the fraction of solubilized azide in DMF, tetrabutylammonium azide (Bu_4NN_3) was added to the reaction mixture. Finally, the temperature of the reaction was increased from 80°C to 120°C. However, none of these alterations resulted in the formation of the wanted product. A possible explanation could be that water interferes with the reaction, however, it was always carried out under nitrogen conditions with freshly dried solvents. Another possible explanation could be that not enough nucleophilic azide was available in DMF. This could be overcome by using trimethylsilyl azide, however, due to the observed low reactivity this was never attempted.

Since with methanesulfonyl activation of the C7 hydroxyl sufficiently high reactivity was not achieved, a triflate, an even stronger leaving group, was applied to activate the free hydroxyl. A triflate group contains three highly electronegative fluorine atoms, further stabilizing the negative charge. Stabilization results in an even weaker base than a methanesulfonyl group, making the triflate an even better leaving group. Installation of the triflate was tried to be achieved by having the free hydroxyl react with trifluoromethanesulfonic anhydride ($(CF_3SO_2)_2O$) with a large base present (Scheme 4). During the first attempt, due to the high reactivity of the reagent, the reaction was carried out in an isopropanol bath at -73°C. After a set amount of time Bu_4NN_3 was added, which was predicted to provide a nucleophilic azide. However, no formation of any product was seen. Another reaction at higher temperature was carried out (-10°C-RT). Due to the high reactivity of $(CF_3SO_2)_2O$), reactions are usually fast. However, after leaving the mixture overnight, primarily starting material remained. Some faint spots appeared on TLC, however, these were difficult to isolate by column chromatography and could not be characterized. The triflate was likely too unstable and thus cleaved on the column during purification.

4.4 Installing an ether bond-linked azide spacer on the C7 hydroxyl

Due to the highly unreactive nature of the C7 hydroxyl the synthesis route of installing an azide directly on the C7 position was sidelined [13]. Instead, investigations into installing a spacer with an azide on the C7 hydroxyl were pursued. This way the C7 hydroxyl would not be utilized as a leaving group, but as a nucleophile. Benefits of installing a spacer were that the stereochemistry would likely not be inverted, thus saving a stereochemistry inversion reaction step. Moreover, a spacer molecule, comprising a primary azide, exhibits higher reactivity compared to a secondary azide in the subsequent click reaction.

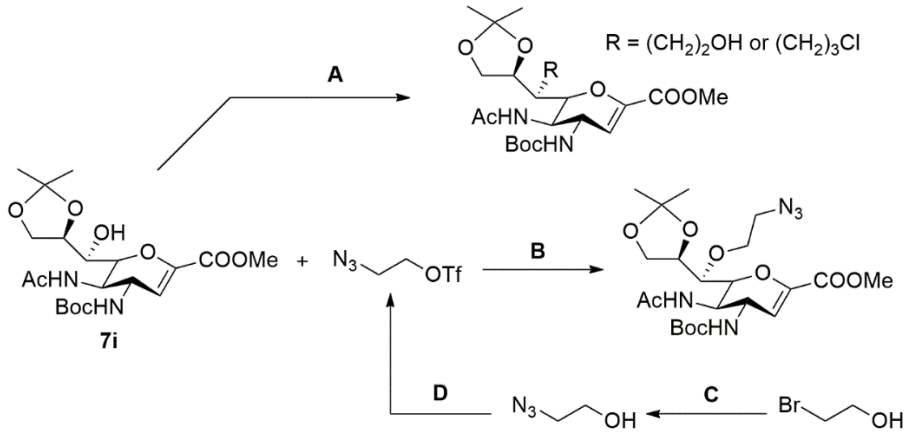

Scheme 5) Different synthesis routes investigated for installing an ether bond azide spacer on the C7 hydroxyl. Conditions: A) 2-Bromoethanol or 1,3-Bromochloropropane, sodium hydride, THF, 0°C-RT, o/n. B) 2-Bromoethanol, Sodium azide, H_2O, 80°, o/n. C) Trifluoromethanesulfonic anhydride, 2,6-Lutidine, DCM, -60°C, 1h. D) Sodium hydride, THF, 0°C-RT, o/n.

Initially, a Williamson ether synthesis was carried out to convert the C7 hydroxyl into an ether bond with a small spacer attached to it. Within this synthesis the C7 hydroxyl was deprotonated using an extremely strong base, sodium hydride, to form an alkoxide. The alkoxide could then perform a nucleophilic attack on an alkyl halide. In this case either 2-bromoethanol or 1,3-bromochloropropane were tried, wherein the bromo-motifs would act as leaving groups (Scheme 5). If the ether bond spacer was successfully installed the resulting terminal hydroxyl or chloro-spacer could then easily be converted into an azide either via a Mitsunobu substitution (hydroxyl) or a S_N2 nucleophilic substitution (chloro). However, all the applied conditions (Table 1) never resulted in conversion, nor the destruction of the starting material. Tetrabutylammonium iodide was added to try and form 2-iodoethanol *in situ*, which should be a better leaving group than a bromide. This, together with a long reaction time, also did not result in the formation of the wanted product. The starting material was always fully recovered after the workup of the reaction. Therefore, the failure of the reaction was not caused by an abundance of H_2O, otherwise sodium hydroxide would form which would deprotect the C1 carboxylic ester. Accordingly, the likely cause for this reaction's failure was that halides are not good enough leaving groups for the low reactivity of the C7 position.

Table 1 Reaction conditions for the three Williamson ether syntheses attempts

Entry	Starting material	Reagent (eq)	Base (eq)	Temperature (°C)	Reaction time	Extra additions
1	**7i**	2-bromoethanol (1.5)	NaH (1)	-20-0-RT	o/n	
2	**7i**	2-bromoethanol (1.5)	NaH (1)	0-RT	72h	TBAI
3	**7i**	1,3-bromochloropropane (2)	NaH (7)	0-RT	4h	

A possible explanation for why the reaction did not occur could be that the bromo halide is not a good enough leaving group for the reactivity of the C7 hydroxyl. Therefore, instead of activating the C7 hydroxyl itself, activation of the spacer leaving group was attempted. First, 2-azidoethanol was successfully synthesized by having 2-bromoethanol undergo a nucleophilic azide attack, substituting the bromo halide for an azide (Scheme 5). Next, the 2-azidoethanol spacer was tried to be activated by installing a triflate group, activating the primary alcohol and forming a highly efficient leaving group. During the first attempt the reaction was followed by TLC, which revealed that 2-azidoethanol had completely disappeared. The reaction mixture was quenched with water, extracted with dichloromethane (DCM) and the remaining crude was directly used in the next reaction. The C7 hydroxyl was deprotonated with NaH and to this mixture the crude activated spacer was added. However, a TLC after 3 hours revealed complete conversion of the SM and a spot on the baseline. Upon further investigation the pH of the reaction mixture, which was expected to be basic, was highly acidic, likely due to remaining trifluoroacetic acid (TfOH) which forms upon quenching the spacer activation reaction with water. The TfOH likely destroyed the SM, resulting in a failed reaction. During the second attempt the spacer activation reaction was quenched with a saturated sodium bicarbonate solution to directly quench the TfOH that forms. Moreover, to gain more insights into what forms during the spacer activation reaction a set of NMR experiments were performed on the crude. These revealed the expected peaks, however, more triplet pairs were observed than expected (Figure 5A). The pairs were identified using Correlated NMR Spectroscopy (COSY) experiments, in which protons that are a maximum of 3-bonds distance from each other reveal a peak on a 2D array. The different pairs suggest the formation of unwanted side products (Figure 5B). Further indicating the formation of unwanted side products were the two peaks seen in the ^{19}F NMR spectrum. Moreover, the ^{19}F peaks reveal similar integration ratios compared to the A and B triplet peaks in the ^{1}H spectrum, suggesting that two triflated molecules were seen in the crude (Figure 5C). A possible explanation for the formation of unwanted side products could be the usage of very old 2-bromoethanol in the synthesis of 2-azidoethanol. However, when the old 2-bromoethanol was checked for purity using NMR the proton and carbon spectra only revealed the expected peaks (Figure S2A/B). It could also be that not all 2-bromoethanol had reacted away during the synthesis of 2-azidoethanol, since it was difficult to visualize 2-bromoethanol on TLC. The remaining 2-bromoethanol could undergo triflation and show up as the second triflated set of triplets on NMR, further interfering with the next reaction.

Since no peaks were observed in the NMR for 2-azidoethanol, the crude was added to the glycal reaction mixture and left to react overnight. Addition of the crude to the glycal resulted in complete disappearance of the SM on TLC. However, unexpectedly only lower running spots were observed on TLC, none of which showed expected peaks on NMR after purification. A methanol flush of the used column gave the sugar product where the methyl ester was hydrolysed. The methyl ester was likely hydrolysed because of sodium hydroxide that formed from NaH when trace amounts of water gets into the reaction mixture. The hetero nuclear single quantum coherence (HSQC) NMR spectrum, wherein carbons that are in close proximity of protons are shown as a peak in a 2D array, of this MeOH flush possibly revealed a CH_2 signal that would only be seen upon spacer addition on the C7 hydroxyl (green box, Figure 4A). However, two peaks would be expected, but only one was seen. Moreover, the ^{19}F NMR spectrum obtained on the MeOH flush also revealed a peak, which was unexpected, but could also be TfOH derivates that also eluted with the MeOH flush. Finally, the obtained NMR spectra were highly impure and thus difficult to interpret properly, making it impossible to confidently say that the spacer was attached.

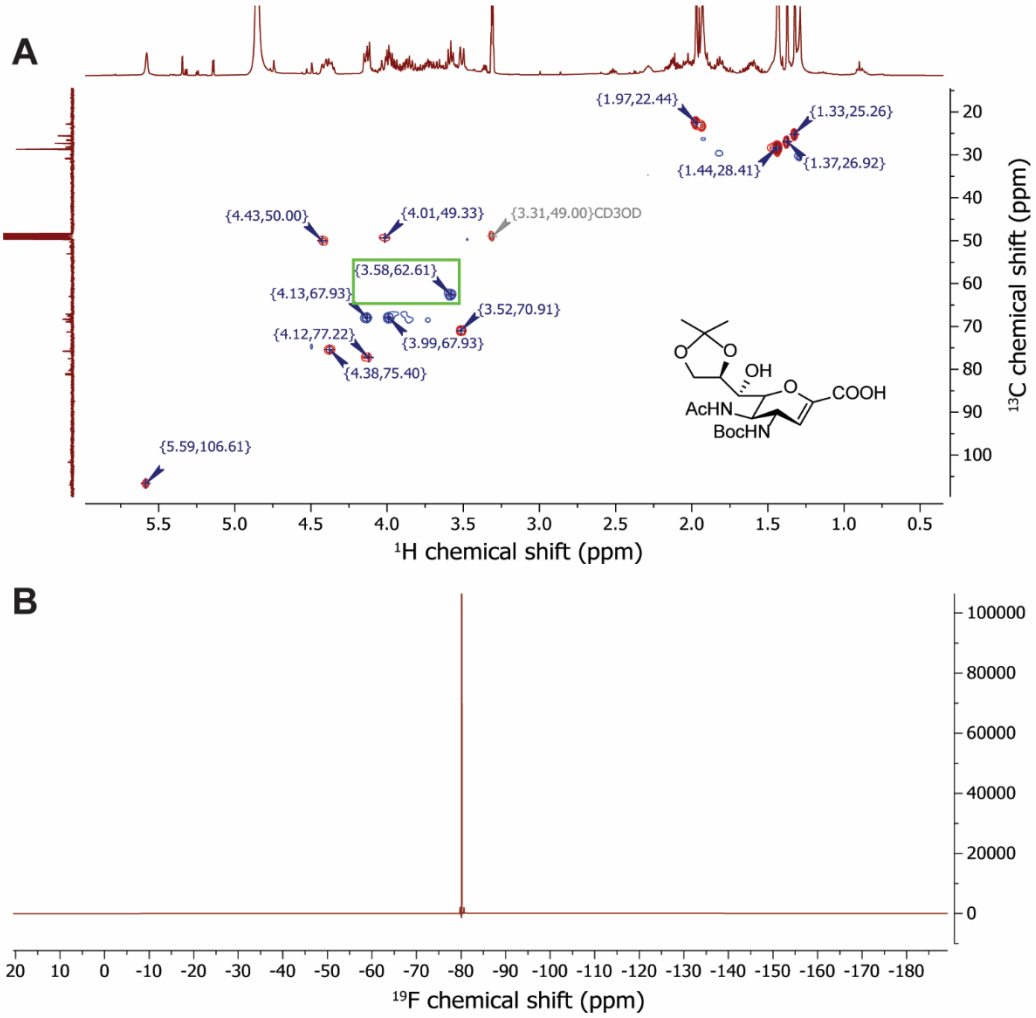

*Figure 4 A) HSQC NMR spectrum of the MeOH flush after addition of the triflated spacer to compound **(7i)**. The missing peak at ~3.80, 52.00 suggests that the methyl ester was cleaved. The green box highlights the peak that could possibly be from an added spacer on the C7 hydroxyl. B) The ^{19}F NMR spectrum of the MeOH flush after addition of the triflated spacer to compound **(7i)**.*

During a third, final, attempt the crude activated spacer would first be purified via a small and quick column chromatography purification. The purification would not only result in the addition of only the triflate activated spacer, but also remove any traces of water. However, the triflate group was likely too reactive, since the activated compound could not be found back in any of the obtained fractions.

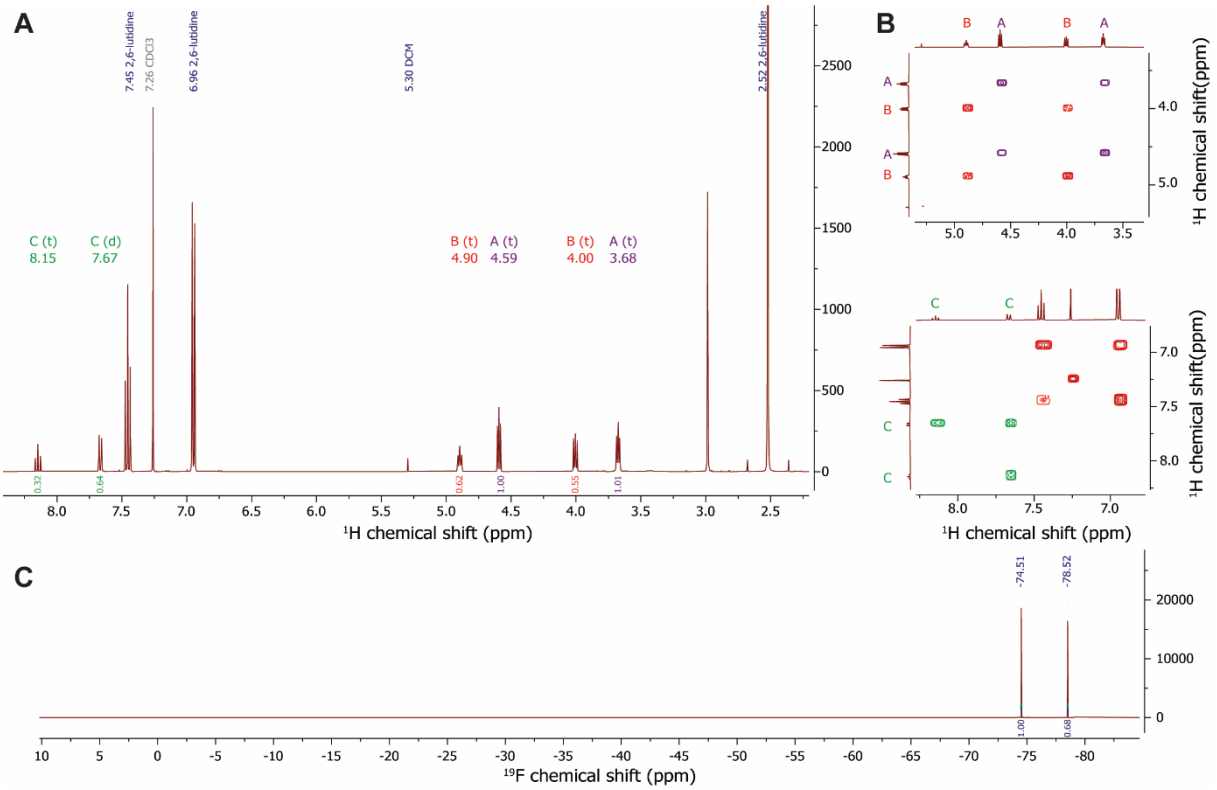

Figure 5 A) ^{1}H NMR spectrum of the crude triflated 2-azidoethanol that reveals multiple triplet sets; A (purple), B (red) and C (green). B) Cutouts of the COSY NMR spectrum of the crude that proved the triplet pairs. C) ^{19}F fluorine NMR spectrum, which reveals two peaks, suggesting the formation of two triflated molecules, likely triplet pairs A and B, as suggested by the integral ratios.

4.5 Installing a carbamate-linked azide spacer on the C7 hydroxyl

Due to the difficulties observed with installing a spacer via an ether bond a different approach was also investigated. A carbamate linker has the general formula $R_2NC(=O)OR$ and displays good chemical and proteolytic stabilities, ideal properties for an ABPP probe. Prior research already highlighted that NAs accept a carbamate linker on the C7 position, since NA inhibition was achieved using this type of linker [14-16]. Within this research two methods for forming a carbamate linker were pursued. Firstly, activating the C7 hydroxyl using 4-nitrophenyl chloroformate in the presence of pyridine was attempted. Here, the oxygen can perform a nucleophilic attack on the carbonyl, ejecting the chlorine as a leaving group. Simultaneously, the pyridine base speeds up the reaction by deprotonating the intermediate. When presenting this activated intermediate with a free amine linked to an azide this would eject the nitrophenyl as a leaving group resulting in the formation of the carbamate linker (Scheme 6).

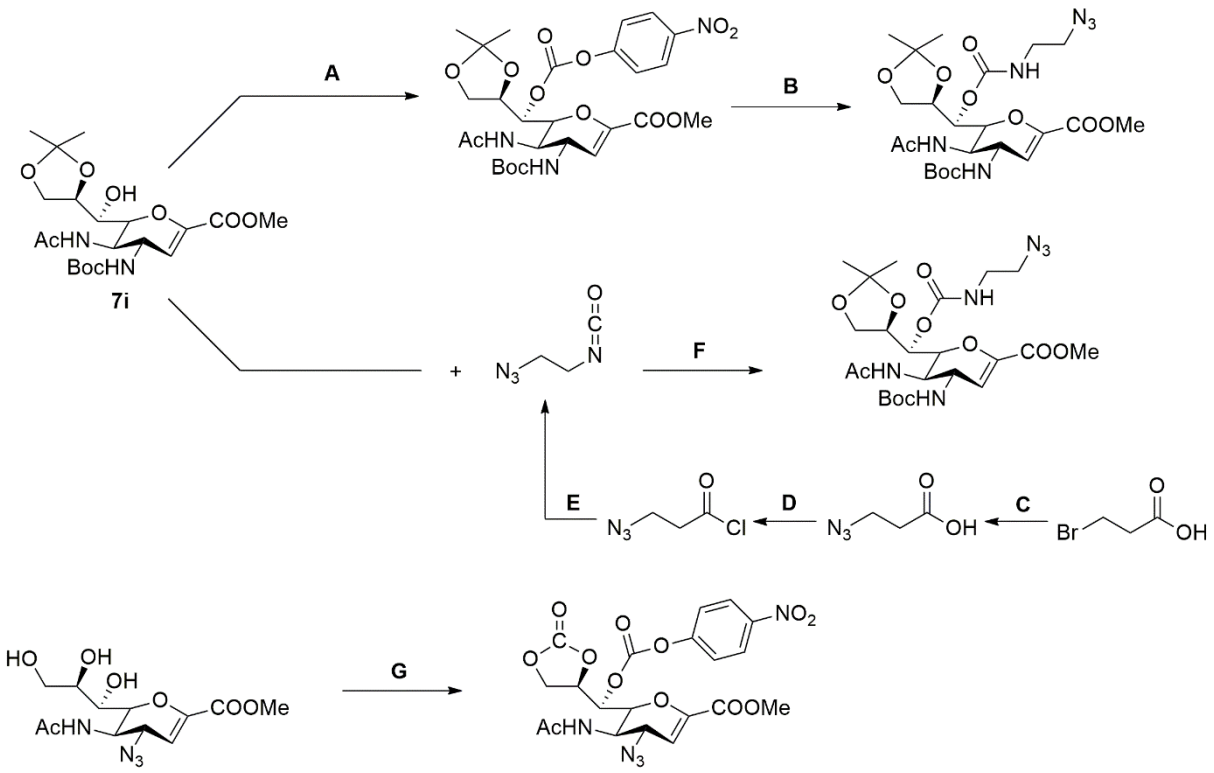

Scheme 6) Different synthesis routes investigated for installing a carbamate azide spacer on the C7 hydroxyl. Conditions: A) 4-Nitrophenyl chloroformate, Pyridine, DMAP, 0°C-RT, o/n. B) 2-Azidoethanamine, Pyridine, DMAP, RT, o/n. C) 3-Bromopropionic acid, Sodium azide, acetonitrile, 85°C, 5h. D) Thionyl chloride, DMF, RT, 3h. E) $TMSN_3$, Toluene, reflux, 2h. F) DMAP, DCM, RT, o/n. G) 4-nitrophenyl chloroformate, DMAP, pyridine, 0°-RT, o/n.

Several attempts, employing different reaction conditions, were made to install a carbamate linker using 4-nitrophenyl chloroformate (Table 2). Initially, all the reagents were directly added together and dissolved in dried pyridine, using activated molecular sieves (4Å), resulting only in the formation of 4-nitrophenol, an unwanted side product. It was believed that too much reagent was added, which resulted in quicker formation of the side product, thus less was added in a second attempt. However, only side product formation was seen, again. Dry DCM was used as solvent, instead of pyridine, in order to reduce the formation of the unwanted side product, which was not observed after 4 hours. However, formation of the wanted product was also not seen after leaving the mixture overnight. Next, a method was found where the reaction was performed on the same molecule as **(7i)** [14]. The procedure was performed exactly as described in the paper, however, only the formation of the unwanted side product was seen. Alternatively, it was theorized that the bulky Boc protection group on the C4 position could also be an issue. Therefore, the same reaction was also tried on **(8ii)** and **(6)**, neither resulting in the desired product. Protection of the C8 and C9 hydroxyls with a carbonyl, while activating the C7 hydroxyl was also considered. Here 4-nitrophenyl chloroformate first activates the C8 or C9 hydroxyl, followed by an intermolecular attack, kicking out nitrophenyl as a good leaving group. Next, more 4-nitrophenyl chloroformate would be added to activate the C7 hydroxyl (Scheme 6). Modest conversion to the carbonyl protected C8 and C9 was seen, however activation of the C7 position was never achieved. All the applied conditions for the different attempts are summarized in table 2.

Table 2 Reaction conditions for the eight attempts at activating the C7 hydroxyl using 4-nitrophenyl chloroformate. The temperature was always 0°C upon addition of the reagents and then heated up to RT. [i] The 4-nitrophenyl chloroformate was added after 30 minutes, as described in [14].

Entry	Starting material	4-nitrophenyl chloroformate eq	DMAP eq	Solvent	Reaction time	Extra additions & notes
1	**7i**	7	7	Pyridine	o/n	
2	**7i**	3.2	3.2	Pyridine	48h	DMAP & 4-nitrophenyl chloroformate 3.2 eq
3	**7i**	2	0.3	DCM	o/n	Pyridine 2.5 eq
4	**7i**	2[i]	2	Pyridine	o/n	
5	**6**	3	3	Pyridine	o/n	
6	**8ii**	3	3	Pyridine	o/n	
7	**5**	1.2 and 2	3.2	Pyridine	2.5h and o/n	C8,9 protection first
8	**7i**	2	2	Pyridine	o/n	CaH dried pyridine

The 4-nitrophenyl chloroformate activation method is described in the literature on exactly the same molecule [14, 15] and on very similar molecules [16, 17]. Therefore, it was expected that this type of C7 hydroxyl activation would be successful. However, upon TLC analysis the SM always remained and only the formation of what would later be proven to be 4-nitrophenol was seen. A small amount of H_2O in the hydroscopic pyridine was believed to be the issue. However, when the used pyridine was distilled over CaH for multiple hours and stored on freshly activated 4Å molsieves the formation of the wanted product was still not seen. The validity of 4-nitrophenyl chloroformate was checked by NMR (Figure S3), which revealed the expected peaks.

Since obtaining a carbamate linker on the C7 position could not be realized using 4-nitrophenyl chloroformate a different route was investigated. An isocyanate-azide linker was considered to add to the C7 hydroxyl for the introduction of the azide group. The C7 hydroxyl could perform a nucleophilic attack on the carbon of the isocyanate, while simultaneously the proton on the hydroxyl shifts to the nitrogen, resulting in the formation of the carbamate linker (Scheme 6). To form the isocyanate-azide linker, 3-azidopropanoic acid was successfully synthesized by having 3-bromopropionic acid subjected to nucleophilic substitution using sodium azide (Figure 6A). Next, the carbonyl was successfully converted into an acyl chloride by a reaction with thionyl chloride in the presence of dimethylformamide (DMF), wherein the DMF acts as a catalyst (Figure 6B). Afterward, an acyl azide was tried to be synthesized by adding $TMSN_3$ to the crude acyl chloride in toluene and refluxing it for two hours. The azide would replace the chlorine, followed by a Curtius rearrangement because of the heat, expelling nitrogen gas and forming an isocyanate (Scheme 6). The acyl azide formation and Curtius rearrangement were attempted twice. A TLC analysis was unavailable due to the high reactivity of acyl chlorides and the difficulty of visualizing them on the plate. Therefore, the reaction was first followed by NMR. However, an NMR of the reaction mixture gave no conclusive answer on whether the isocyanate had actually been formed. In the proton NMR, it was expected to see a set of triplet peaks, as was seen for the acyl chloride. However, multiple sets were seen, raising the question whether unwanted side products were formed (Figure 6B/C). Since the reaction was performed in toluene, these were the main solvent peaks seen, increasing the difficulty of spectrum interpretation. Moreover, no reference spectra were available for 1-azido-2-isocyanateoethane, thus a comparison was unavailable. Next, infrared (IR) spectroscopy was applied to try and prove that an isocyanate was present in the reaction mixture. Isocyanates reveal a characteristic peak between 2275-2250 cm^{-1} for the N=C=O bonds. However, azides reveal a characteristic peak between 2160-2120 cm^{-1}, problematically close. In the IR spectrum a broad signal that might be showing two peaks was seen in

the 2300-2100 cm^{-1} region (green box, Figure 6D). These peaks could correspond to both an azide and an isocyanate, but it could also be that one corresponds to an azide on 3-azidopropanoyl chloride (or a derivate thereof) and an azide of excess $TMSN_3$.

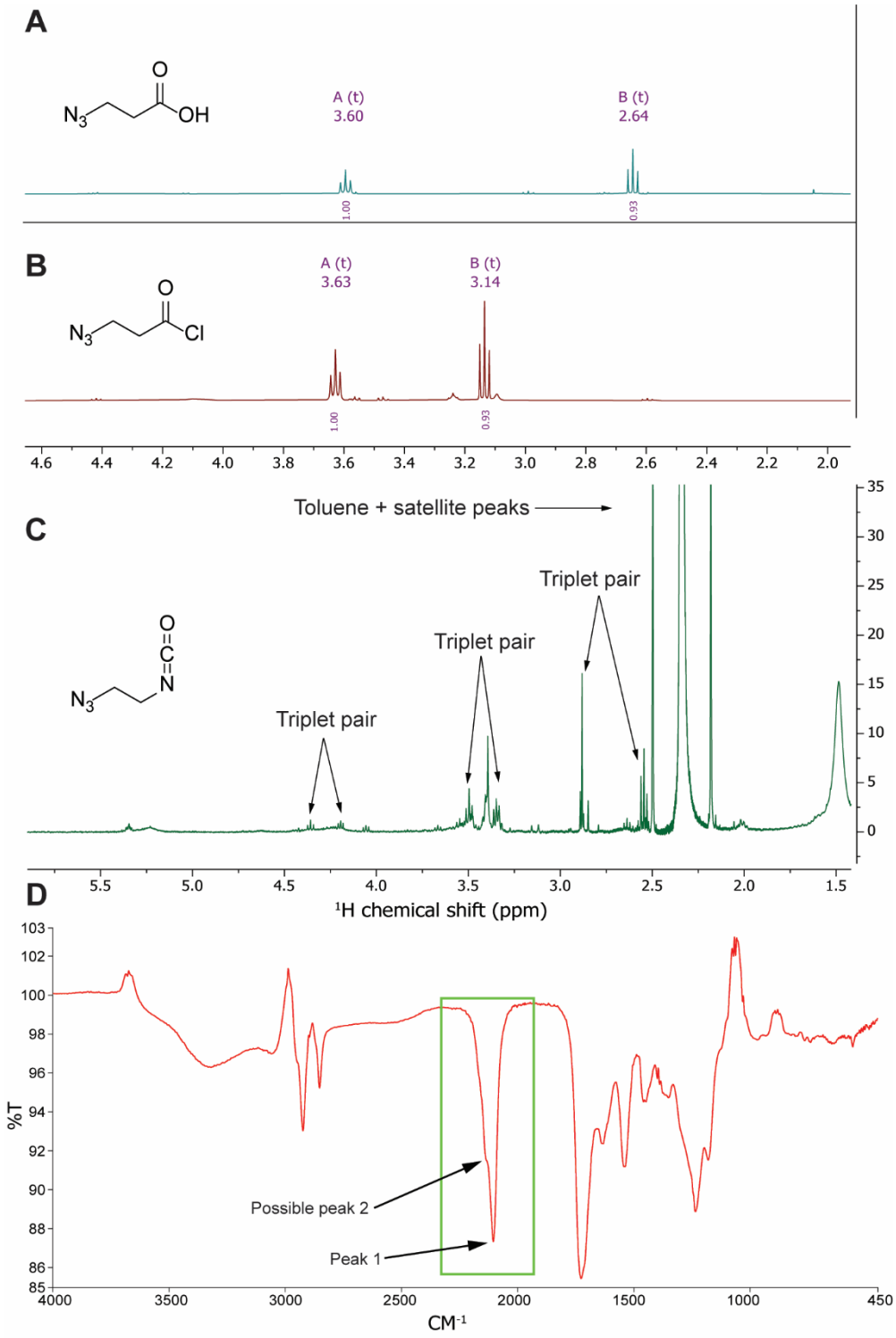

Figure 6 A) ^{1}H NMR spectrum of 3-azidopropionic acid. B) ^{1}H NMR spectrum of 3-azidopropanoyl chloride. C) ^{1}H NMR spectrum of the reaction mixture for the synthesis of 1-azido-2-isocyanateoethane. Multiple triplet pairs were observed, while no triplet pair was seen for 3-azidopropanoyl chloride. D) Obtained IR spectrum of the 1-azido-2-isocyanateoethane reaction mixture with the 2300-2100 cm^{-1} region highlighted in a green box. The two peaks are annotated by arrows.

Nevertheless, in the proton NMR of the isocyanate crude mixture a triplet pair for 3-azidopropanoyl chloride could not be seen, thus compound **(7i)** was added to the crude. However, after leaving the reaction overnight no conversion was seen, further casting doubts over the reactivity of the C7 hydroxyl and the validity of the synthesized molecules. To test the reactivity of the C7 hydroxyl an available isocyanate, ethyl isocyanate, was also added to compound **(7i)**, on a small scale. Here it was known that the isocyanate was present, as proven by NMR (Figure S4). However, no conversion to the corresponding C7 carbamate was seen on TLC. Further questioning whether the C7 hydroxyl is reactive enough and whether compound **(7i)** is the compound that it is thought to be. Furthermore, since the isocyanate reaction, and the activation of the C7 hydroxyl for a carbamate linker using 4-nitrophenyl chloroformate, have already been performed on a very similar molecule (protected Zanamivir, [18]) and on exactly the same molecule [14], respectively, it raises the question what was causing all the failed reactions.

4.6 Installing the difluoro motif before the clickable tag

A comparison of the three dimensional (3D) conformations of unprotected difluoro sialic acid and sialic acid where the double bond is still present between C2 and C3 reveals highly different 3D structures. The 3D structures were simulated by MM2 energy minimization for each molecule (Figure 7A/B).

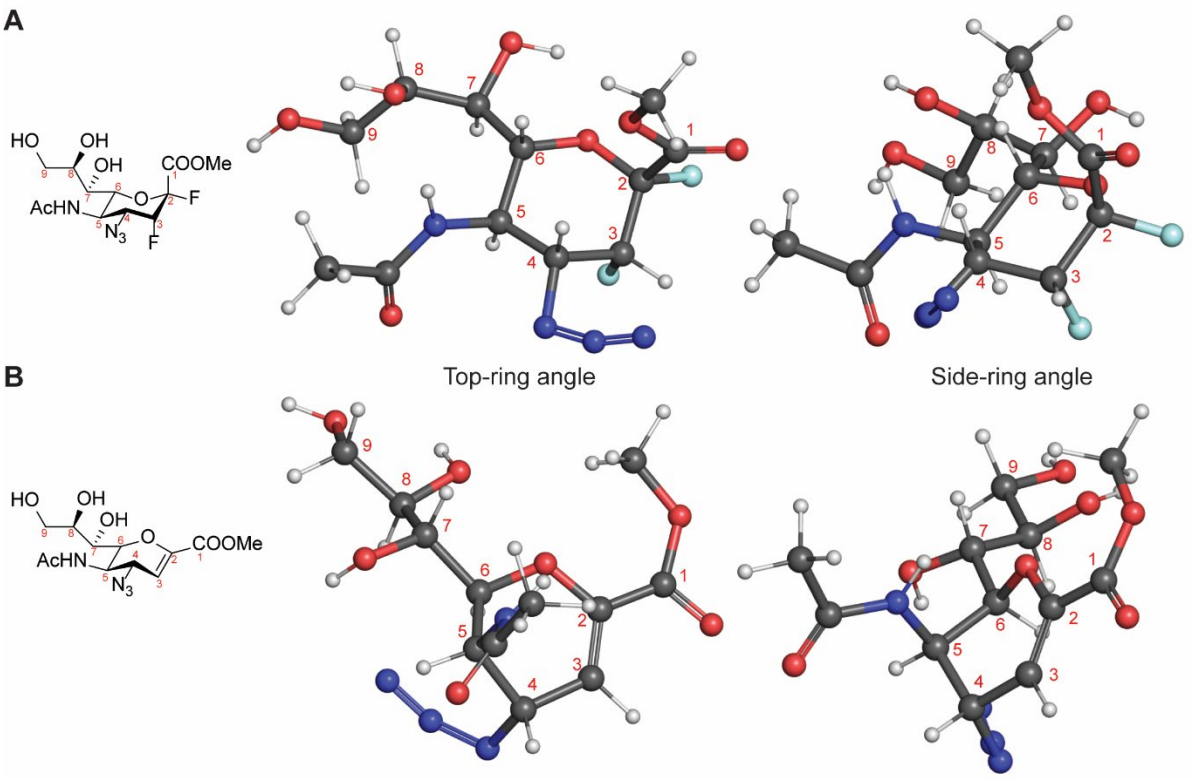

Figure 7 A) Simulated 3D structure of difluoro sialic acid. B) Simulated 3D structure of sialic acid where the double bond is still present between C2 and C3. The molecules differentiate in angles of ring attachments and the 3D shape of the ring itself. MM2 energy minimization was performed for both small molecules.

Different conformations could have a significant impact on the reactivity of molecules. Therefore, attempts were made at first installing the difluoro motif and next adding a clickable tag on the C7 position. First, **(4)** underwent electrophilic fluorination on the C3 position using SelectFluor® [19]. The reaction resulted in expected yields and the formation of axial (ax) and equatorial (eq) isomers. Both isomers are known to bind to NAs covalently, thus both isomers underwent fluorination on the C2 position [8]. The C2 hydroxyl was substituted for a fluorine using diethylaminosulfur trifluoride (DAST). The C3-F axial isomer saw the formation of both C2-F equatorial and C2-F axial isomers in an

approximately 6:1 ratio. This was likely because DAST can react via both S_N1 (stereochemistry retaining) and S_N2 (stereochemistry inversion) mechanisms. While S_N2 is preferred, S_N1 can also be observed when this is not sterically hindered. The formation of the C2-F axial isomer was not seen for the C3-F equatorial isomer, likely because the C3-F in the equatorial position sterically hinders the S_N1 reaction mechanism. The reactions resulted in the expected yields and are in accordance with the literature [8] (Scheme 7).

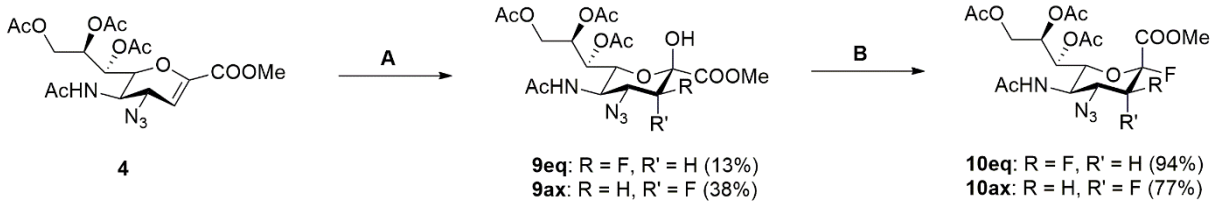

Scheme 7) Synthesis route for the instalment of the difluoro motif on C2 and C3 of sialic acid. Conditions: A) Selectfluor®, nitromethane/H2O (5:1), RT-50°C, o/n. B) Diethylaminesulfur trifluoride (DAST), DCM, -40°C-RT, 0.5h.

Before the instalment of a spacer could be tested on difluoro sialic acid, the *O*-acetyl groups were removed using sodium methoxide or sodium in dry methanol. However, opportunistic H_2O likely caused the formation of sodium hydroxide, resulting in the hydrolysis of the methyl ester and forming compound **(11eq)** and **(11ax)**. Since, the C2-F was labile to acid the standard conditions for installing the methyl ester could not be applied. Therefore, TMS-diazomethane was used. TMS-diazomethane was protonated by the carboxylic acid, forming a carboxylate. Next, the carboxylate performed a nucleophilic attack on the partially positively charged methyl group, reinstalling the methyl ester and displacing nitrogen gas. TMS-diazomethane successfully reinstalled the methyl ester with expected yields, resulting in compound **(12eq)** and **(12ax)** (Scheme 8).

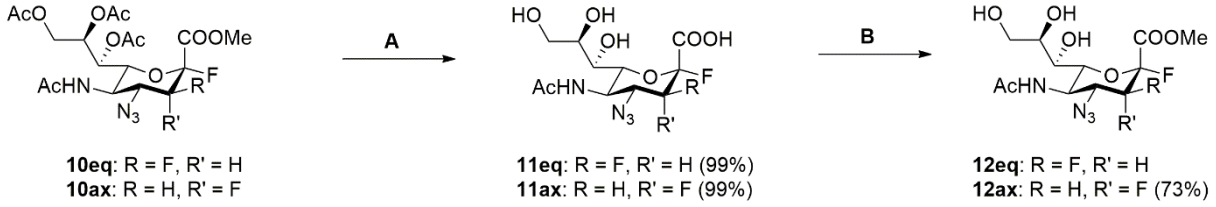

Scheme 8) Synthesis route for the O-acetyl deprotection and reinstalment of the methyl ester. Conditions: A) Sodium methoxide/Sodium(s), MeOH, H^+, RT, 3h. B) Trimethylsilyldiazomethane, MeOH/toluene (1:1), 0°C-RT, o/n.

With the 3D conformation significantly changed in compounds **(12eq)** and **(12ax)** compared to the glycal structure of compound **(7i)**, the C8 and C9 protection and C7 activation using 4-nitrophenyl chloroformate was attempted twice (Scheme 9).

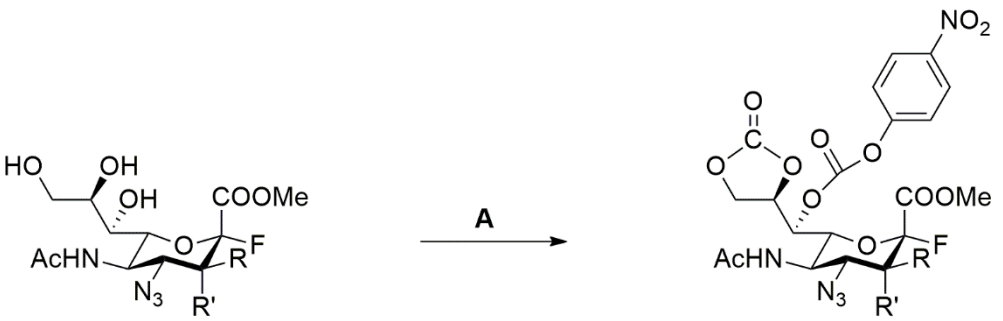

12eq: R = F, R' = H
12ax: R = H, R' = F

13eq: R = F, R' = H
13ax: R = H, R' = F

Scheme 9) Reaction conditions for C8 and C9 carbonyl protection and C7 hydroxyl activation on difluoro sialic acid. Conditions: A) 4-nitrophenyl chloroformate, DMAP, pyridine, 0°-RT, o/n.

At first, the C8 and C9 carbonyl protection, again, saw modest conversion, but the main product that formed was 4-nitrophenol. Upon the addition of more 4-nitrophenyl chloroformate, neither more conversion to C8 and C9 protected, nor the formation of C7 activated compound was observed, except the formation of more 4-nitrophenol. Previous observations by our group on reactions with 4-nitrophenyl chloroformate disclosed that the concentration of the reaction mixture plays a significant role. Therefore, during the second attempt a 0.3M reaction mixture was employed, which resulted in a very small amount of pyridine. To ensure proper stirring, a heart shaped flask was used. However, the higher reaction mixture concentration did not result in the wanted compound and the same was observed as in the previous attempt. None of the attempted reactions resulted in the attachment of a clickable tag on the C7 position of sialic acid. All the used reagents quality were tested using NMR and no issues or impurities were found. This raised the question why nothing can be attached or substituted onto the C7 hydroxyl position. A possible explanation could be that unseen impurities have side reactions with the reagents, perturbing the reaction. Extraordinary effort was always taken to work under water-free conditions, however, fully diminishing every H_2O molecule is virtually impossible. These sporadic H_2O molecules could have interfered with the reaction. However, salts, metals or other non-organic impurities, that are invisible to standard proton and carbon NMR techniques, could also have a significant impact on reactions and reagents. Moreover, different literature describes several modifications on the C7 hydroxyl position on the same [14, 15] or very similar molecules [16-18, 20], questioning whether the synthesized molecule actually is what it is thought be.

5 General discussion, conclusion and outlook

The influenza virus causes a common acute respiratory infection that can be dangerous to young children, immunocompromised individuals and adults aged 65 years and older [5, 6]. Sialidases play a key role in the infection cycle of the influenza virus. Gaining a greater understanding of sialidase activity can be essential for further elucidating the workings of the virus. Sialidases bind to terminal sialic acids on glycoconjugates located in the cellular envelope [4]. This makes sialic acid a perfect candidate for an ABPP probe that reports on sialidase activity. ABPP probes report on their target by binding specifically and incorporating a tag that can be used as a reporter or affinity label. Chemical modification of sialic acid ensures a long-lasting covalent bond, critical for ABPP probing. By installing a fluorine on the C2 and C3 position of sialic acid this can be achieved. The fluorine on the C3 position destabilizes the transition state, limiting the rate of hydrolysis. Conversely, the fluorine on the C2 position speeds up the formation of the bond between sialidases and sialic acid by being a good leaving group [8]. Sialidase ABPP probes containing a fluorine on the C2 and C3 position have already been realised [10]. However, these probes possess the reporter tag on a carbon which causes the loss of an important interaction within the active site of sialidases. The C7 hydroxyl is known to not have any interaction with residues of sialidases, thus placing the reporter tag here would theoretically result in greater binding affinities for the probe [8]. Therefore, an attempt was made to synthesize a sialidase ABPP probe starting from sialic acid, containing the reporter tag on the C7 position and the difluoro motif for covalent long-lasting binding.

As was already discussed with the results, none of the attempted reactions resulted in the placement of a clickable tag on the C7 position of sialic acid. Nevertheless, highly similar modifications on the C7 position have already been described within the literature, raising the question whether compound **(7i)** was synthesized correctly. The validity of compound **(7i)** was first reviewed by comparing the measured proton NMR shifts with the shifts reported in: [14]. The reported shifts were identical to what was measured, suggesting that compound **(7i)** was synthesized correctly. Furthermore, a high-resolution mass spectrometry (HR-MS) measurement on compound **(7i)** revealed a $[M\text{-}Na]^+$ mass of 467.2002 ,while the calculated $[M\text{-}Na]^+$ mass was 467.2000, further proving that the correct compound was synthesized. Therefore, other impurities, together with the extremely low reactivity of the C7 position of sialic acid, were likely the cause of the failed reactions to activate the C7 position of sialic acid.

Alternative approaches that have not yet been tried were theorized, since the clickable tag on the C7 position could not be realized. Firstly, further optimization of the reaction wherein an ether-bond spacer was activated by triflation could yield the wanted product, since this was possibly already observed on a small scale (Figure 4A). First, the triflation of the spacer should be optimized by making sure only the wanted triplet peak set is observed in proton NMR (Figure 5A). Next, the addition of the activated spacer to the reaction mixture likely contained too much moisture, hydrolysing the methyl ester. An effective way of removing moisture before addition has to be found to eliminate methyl ester hydrolysis.

Installing a carbamate linker on the C7 position of sialic acid was described in the literature many times previously, therefore, it should be investigated further. Moreover, previously it was already successfully performed by members of our group. Applying an alternative base, such as triethylamine, could possibly mitigate the formation of 4-nitrophenol. Furthermore, another purification step of the starting material, recrystallization for instance, could potentially remove theoretical unseen impurities that interfere with the reaction. Finally, applying Schlenk-conditions could dispose of sporadic H_2O, which is favourable for the success of the reaction.

Finally, investigating a chemoenzymatic approach could result in the attachment of the clickable tag on the C7 position. Khedri et al. (2014) describe a one-pot three-enzyme synthesis of sialosides containing C7-modified sialic acids, including an azide, starting from chemically modified ManNAc [21]. The sialoside could then undergo enzymatic cleavage to liberate the C7 modified sialic acid. Once the probe is obtained, its inhibition activity on viral NAs will be determined by fluorescence-based enzyme inhibition assays. The labelling properties will be tested on both recombinant viral NA and intact virus particles.

6 Materials and Methods

6.1 General information

All used chemicals were of analytical grade and purchased from reputable companies. When indicated, solvents were dried and stored over activated 4Å molecular sieves. MeOH was dried and stored over activated 3Å molecular sieves. Reactions were followed using aluminium- or glass-backed Silica Gel ($60F_{254}$) thin layer chromatography (TLC) plates with a thickness of 0.2mm (SILICYCLE). Carbohydrates were visualized using a H_2SO_4 in EtOH solution (5% v/v) or, when possible, UV light (254 nm). Column chromatography was performed on VWR chemicals silica gel 60 (40-63 µm mesh) using distilled solvents. Proton, carbon and fluorine NMR spectra were recorded on a Agilent Technologies 400 MHz Fourier Transform spectrometer equipped with a 5 mm probe or Bruker 600 MHz Ultrashield Fourier Transform spectrometer fitted with a 5 mm cryoprobe. All spectra were referenced using the residual solvent peak for their respective solvents. Coupling constants (*J*) were given in Hertz (Hz). Carbon NMR spectra were performed with broadband proton decoupling. COSY and HSQC two-dimensional spectra were recorded and used to aid the assignment of peaks to their respective compounds. High Resolution Mass Spectrometry (HRMS) was recorded on an Agilent Technologies 6560 ion mobility Q-TOF.

6.2 Methyl (5-acetamido-3,5-dideoxy-D-glycero-α-D-galacto-2-nonulopyranosid)onate (1)

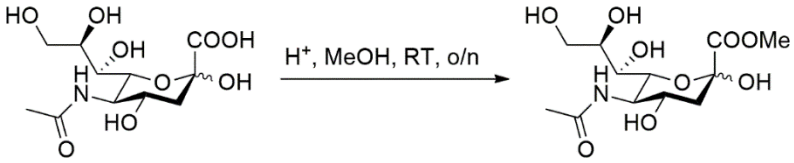

Neu5Ac **1**

N-acetylneuraminic acid (2.24 g, 7.24 mmol) and Amberlite IR-120 (3.51 g) were dissolved in MeOH (100 ml) and left to stir overnight at RT. The progress of the reaction was monitored by TLC (EtOAc/MeOH/H_2O, 7:2:1) and upon completion the mixture was filtered and concentrated to obtain the crude as a yellow foam-like solid **(1)**.

6.2 Methyl (5-acetamido-2,4,7,8,9-penta-*O*-acetyl-3,5-dideoxy-D-glycero-α-D-galacto-2-nonulopyranosid)onate (2)

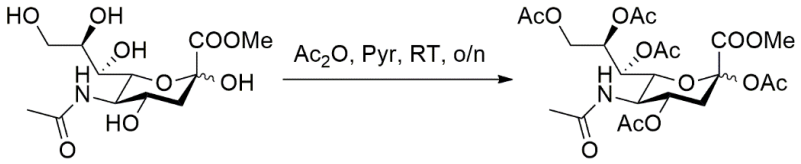

1 **2**

The crude starting material **(1)** (2.30 g, 7.11 mmol) was dissolved in pyridine (5 ml) and acetic anhydride (9 ml) and left stirring overnight at RT. TLC was used to monitor the reaction (EtOAc) and upon completion the solvent was removed by evaporation. Traces of pyridine were removed via co-evaporation with toluene. The crude was further purified by column chromatography (EtOAc) to obtain **(2)** as a yellow foam-like solid (1.98 g, 52% yield).

6.3 2-Methyl-4,5-dihydro-(methyl(7,8,9-tri-*O*-acetyl-2,6-anhydro-3,4,5-trideoxy-D-glycero-D-talo-non-2-en)onate)[5,4-d]-1,3-oxazole (3)

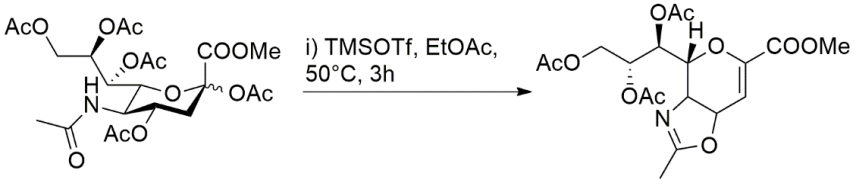

2 **3**

To a solution of **(2)** (9.02 g, 16.91 mmol) in EtOAc (100 ml) was added trimethylsilyl trifluoromethanesulfonate (10 g, 44.99 mmol), dropwise over 10 minutes and the mixture was heated to 50°C under nitrogen. After 3 hours TLC revealed completion of the reaction and it was quenched by transferring to a saturated sodium bicarbonate solution (100 ml) on ice and stirring it for 10 minutes. Next, the mixture was extracted with EtOAc (2x 100 ml) and the combined organic layers were washed with brine (2 x 100 ml), dried with Na_2SO_4 and concentrated. The wanted product **(3)** was further purified by column chromatography (EtOAc/PE, 8:2) and obtained as a foamy white solid (4.67 g, 67% yield). ^{1}H NMR (400 MHz, $CDCl_3$) δ 6.39 (d, *J* = 4.0 Hz, 1H, H3), 5.64 (dd, *J* = 5.9, 2.6 Hz, 1H, H7), 5.45 (td, *J* = 6.2, 2.6 Hz, 1H, H8), 4.82 (dd, *J* = 8.6, 4.0 Hz, 1H, H4), 4.60 (dd, *J* = 12.5, 2.6 Hz, 1H, H9'), 4.23 (dd, *J* = 12.5, 6.4 Hz, 1H, H9"), 3.96 (tt, *J* = 9.7, 1.1 Hz, 1H, H5), 3.82 (s, 3H, $COOCH_3$), 3.44 (dd, *J* = 10.1, 2.6 Hz, 1H, H6), 2.16 (s, 3H, CH_3), 2.06 (s, 3H, CH_3), 2.06 (s, 3H, CH_3), 2.01 (d, 3H, CH_3). ^{13}C NMR (101 MHz, $CDCl_3$) δ 170.80 (C=O), 169.95 (C=O), 169.72 (C=O), 167.31 (N=C-O), 162.03 (C1), 147.32 (C2), 107.72 (C3), 76.92 (C6), 72.39 (C4), 70.45 (C7), 69.03 (C8), 62.24 (C9), 62.15 (C5), 52.69 (O-CH_3), 21.00, 20.93, 20.77, 14.33, 14.30 (4 x CH_3).

6.4 Methyl 5-acetamido-7,8,9-tri-*O*-acetyl-2,6-anhydro-4-azido-3,4,5-trideoxy-D-glycero-D-galacto-non-2-enonate (4)

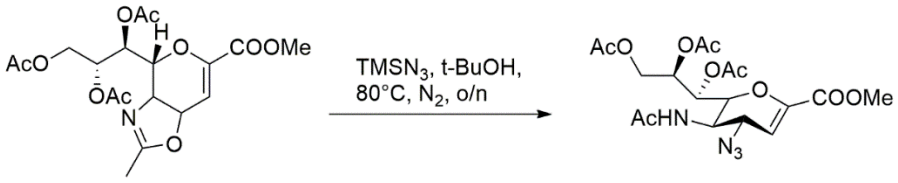

3 **4**

To a solution of **(3)** (4.67 g, 11.30 mmol) in tert-butanol (100 ml) under nitrogen was slowly added azidotrimethylsilane (3.4 ml, 24.87 mmol). The mixture was refluxed (80°C) overnight. Upon completion (monitored by TLC) the reaction was quenched by adding an aqueous sodium nitrite solution (5.33 g in 26 ml H_2O). Next, 6M HCl was added dropwise until effervescence stopped. The mixture was diluted with EtOAc (150 ml) and H_2O and washed with H_2O (2 x 100 ml). Aqueous layers were combined and extracted with EtOAc (2 x 60 ml). Organic layers were combined and washed with saturated $NaHCO_3$ (100 ml), brine (150 ml), dried with Na_2SO_4 and concentrated *in vacuo* to obtain crude product **(4)** without further purification as a yellow foam-like solid (5.11 g, 99% yield). ^{1}H NMR (400 MHz, $CDCl_3$) δ 5.98 (d, *J* = 2.8 Hz, 1H, H3), 5.65 (d, *J* = 8.6 Hz, 1H, NH), 5.45 (dd, *J* = 5.6, 2.5 Hz, 1H, H7), 5.35 (ddd, *J* = 6.3, 5.6, 2.8 Hz, 1H, H8), 4.59 (dd, *J* = 12.4, 2.8 Hz, 1H, H9'), 4.53 (ddd, *J* = 8.7, 7.9, 2.7 Hz, 1H, H4), 4.20 (dd, *J* = 12.4, 6.4 Hz, 1H, H9"), 3.81 (s, 3H, $COOCH_3$), 3.78 (dt, *J* = 9.8, 8.6 Hz, 1H, H5), 2.14 (s, 3H, CH_3), 2.06 (d, *J* = 8.6 Hz, 6H, 2 x CH_3), 2.01 (s, 3H, CH_3). ^{13}C NMR (101 MHz, $CDCl_3$) δ 170.71 (2 x C=O), 170.59 (C=O), 170.15 (C=O), 161.64 (C1), 145.32 (C2), 107.54 (C3), 75.62 (C6), 70.63 (C8), 67.88 (C7), 62.07 (C9), 57.44 (C4), 52.76 (O-CH_3), 49.18 (C5), 23.56 (CH_3), 21.04 (CH_3), 20.94 (CH_3), 20.88 (CH_3).

6.5 Methyl 5-amino-7,8,9-tri-hydroxy-2,6-anhydro-4-azido-3,4,5-trideoxy-D-glycero-D-galacto-non-2-enonate (5)

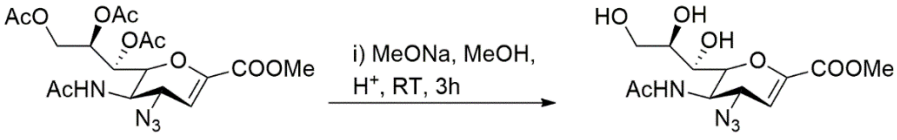

4 **5**

The starting material **(4)** (0.95 g, 2.08 mmol) dissolved in dry MeOH (30 ml) was stirred under nitrogen. Next, sodium methoxide (0.0345 g, 0.62 mmol) dissolved in dry MeOH (5 ml) was added to the mixture while on ice. After five more minutes on ice the mixture was left to react at RT for approximately 3 hours (reaction was monitored by TLC). Upon completion the mixture was neutralized using Amberlite IR-120, filtered and the solvent evaporated to obtain the final product **(5)** as a white solid (0.65 g, 95% yield). ^{1}H NMR (400 MHz, CD_3OD) δ 5.93 (d, *J* = 2.5 Hz, 1H, H3), 4.35 (dd, *J* = 9.4, 2.5 Hz, 1H, H4), 4.28 (dd, *J* = 10.8, 1.3 Hz, 1H, H6), 4.13 (dd, *J* = 10.8, 9.4 Hz, 1H, H5), 3.89 (dd, 1H, H8), 3.85 (dd, 1H, H9"), 3.80 (s, 3H $COOCH_3$), 3.67 (dd, *J* = 11.4, 5.3 Hz, 1H, H9'), 3.61 (dd, *J* = 9.4, 1.2 Hz, 1H, H7), 2.03 (s, 3H, CH_3). ^{13}C NMR (101 MHz, CD_3OD) δ 174.45 (C=O), 163.78 (C=O), 146.90 (C1), 108.34 (C2), 78.13 (C6), 71.10 (C8), 69.66 (C7), 64.80 (C9), 59.78 (C4), 52.95 (O-CH_3), 49.21 (C5), 22.70 (CH_3).

6.6 Methyl 5-acetamido-2,6-anhydro-4-azido-3,4,5-trideoxy-8,9-*O*-isopropylidene-D-glycero-D-galacto-non-2-enonic acid (6)

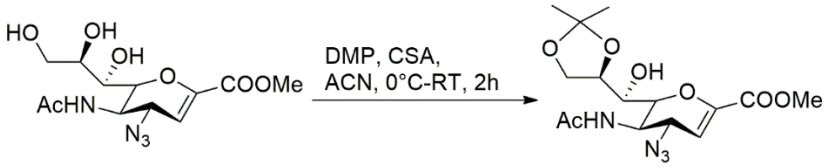

5 **6**

To a solution of **(5)** (0.57 g, 1.726 mmol) in dry acetonitrile (55 ml) was added camphorsulfuric acid (0.344 g, 1.381 mmol) in dry acetonitrile (8 ml) and 2,2-dimethoxy propane (0.4 ml 2.589 mmol) at 0°C. The mixture was stirred at this temperature for five more minutes before gradually warming to RT, reacted for three hours (reaction was monitored with TLC). Upon completion the reaction was quenched using triethylamine (4 ml) and concentrated *in vacuo*. The crude was further purified by column chromatography (EtOAc/PE, 75:25) to obtain product **(6)** as a white solid (0.59 g, 92% yield). ^{1}H NMR (400 MHz, CD3OD) δ 5.93 (d, *J* = 2.5 Hz, 1H, H3), 4.36 (dd, *J* = 9.3, 2.5 Hz, 1H, H4), 4.33 – 4.27 (m, 1H, H8), 4.19 (dd, *J* = 10.8, 1.3 Hz, 1H, H6), 4.13 (dd, *J* = 5.9, 2.8 Hz, 1H, H9"), 4.11 – 4.08 (m, 1H, H5), 4.01 (dd, *J* = 8.7, 5.3 Hz, 1H, H9'), 3.80 (s, 3H, $COOCH_3$), 3.62 (dd, *J* = 7.8, 1.2 Hz, 1H, H7), 2.03 (s, 3H, CH_3), 1.37 (s, 3H, CH_3), 1.33 (s, 2H, CH_3). ^{13}C NMR (101 MHz, CD_3OD) δ 174.22 (C=O), 163.47 (C=O), 146.75 (C2), 110.31 ($(CH_3)_2C$-$(O)_2$), 108.48 (C3), 78.42 (C6), 76.09 (C8), 70.49 (C7), 67.88 (C9), 59.60 (C5), 52.97 (O-CH_3), 49.53 (C5), 27.20 (CH_3), 25.58 (CH_3), 22.73 (CH_3).

6.7 Methyl 5-acetamido-2,6-anhydro-4-[(tert-butoxycarbonyl)amino]-3,4,5-trideoxy-8,9-*O*-(1-methylethylidene)-D-erythro-non-2-enonate (7i)

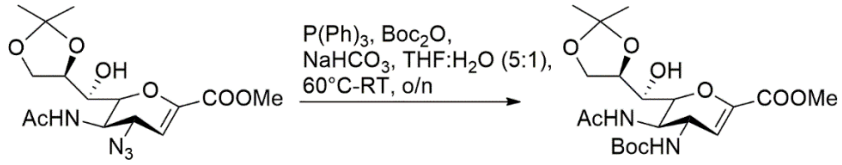

6 **7i**

The starting material **(6)** (0.1573 g, 0.425 mmol) and triphenylphosphine (0.32 g, 1.193 mmol) were dissolved in THF:H_2O (5:1, v/v, 12 ml) and heated to 60°C. After 2 hours the mixture was cooled to RT and treated with $NaHCO_3$ (0.08 g, 0.849 mmol) and di-tert-butyl dicarbonate (0.19 g, 0.849 mmol) successively, and left to react overnight. Upon completion (monitored by TLC) the reaction was diluted with H_2O (20 ml) and extracted with EtOAc (3 x 20 ml). The organic layers were combined and washed with 1M HCl (aq, 25 ml), $NaHCO_3$ (sat. aq. 25 ml), brine (25 ml), dried with Na_2SO_4, filtered and concentrated *in vacuo*. The crude was further purified by column chromatography (EtOAc/PE, 5:5 – 8:2) to obtain the product **(7i)** as a white solid (0.12 g, 64% yield). ^{1}H NMR (400 MHz, $CDCl_3$) δ 6.67 (d, *J* = 6.5 Hz, 1H, NH), 5.80 (d, *J* = 2.3 Hz, 1H, H3), 5.08 (d, *J* = 4.3 Hz, 1H, OH), 4.87 (d, *J* = 9.0 Hz, 1H, NH), 4.59 (td, *J* = 9.4, 2.4 Hz, 1H, H4), 4.42 – 4.33 (m, 1H, H8), 4.19 – 4.06 (m, 2H, H9" H9'), 4.01 (d, *J* = 10.6 Hz, 1H, H6), 3.91 (td, *J* = 10.1, 6.5 Hz, 1H, H5), 3.76 (s, 3H, $COOCH_3$), 3.50 (dd, 1H, H7), 2.03 (s, 3H, CH_3), 1.44 (s, 9H, 3 x CH_3), 1.40 (s, 3H, CH_3), 1.36 (s, 3H, CH_3). ^{13}C NMR (101 MHz, $CDCl_3$) δ 174.03 (C=O), 162.19 (C=O), 157.31 (C=O), 146.41 (C2), 109.34 ($(CH_3)_2C$-$(O)_2$), 108.05 (C3), 81.13 ($C(CH_3)_3$), 78.40 (C6), 74.16 (C8), 69.86 (C7), 67.47 (C9), 52.51 (O-CH_3), 52.10 (C5), 48.83 (C4), 28.33 (3 x CH_3), 27.22 (CH_3), 25.41 (CH_3), 23.16 (CH_3).

6.8 Methyl 5-acetamido-2,6-anhydro-7-[(2,2,2trifluoroacetoxy)methyl]-4-[2,2,2-trifluoroacetamido]-3,4,5-trideoxy-8,9-*O*-(1-methylethylidene)-D-erythro-non-2-enonate (7ii)

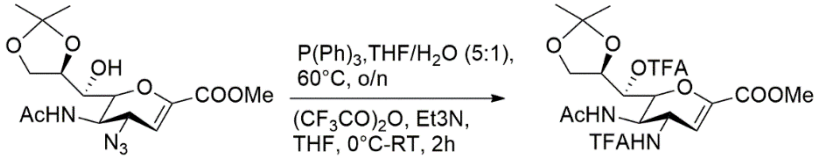

6 **7ii**

Compound **(6)** (0.0512 g, 0.138 mmol) and triphenylphosphine (0.102 g, 0.388 mmol) were dissolved in THF:H_2O (5:1, v/v, 10 ml), heated to 60°C and stirred overnight. The solvent was removed by co-evaporation with toluene. The remaining crude was directly dissolved in THF (3 ml) and treated with triethylamine (0.056 ml, 0.403 mmol) and trifluoroacetic anhydride (0.033 ml, 0.233 mmol) under nitrogen atmosphere. After two hours the reaction was quenched with H_2O and extracted with EtOAc (3 x 20 ml). The organic layers were combined, washed with brine (25 ml), dried with Na_2SO_4, filtered and concentrated *in vacuo*. The crude was further purified by column chromatography (EtOAc/PE, 5:5-100% EtOAc) to obtain the product **(7ii)** as a white solid (0.027 g, 40% yield). ^{1}H NMR (600 MHz, $CDCl_3$) δ 8.26 (d, J = 9.2 Hz, 1H, NH), 6.69 (d, J = 8.8 Hz, 1H, NH), 5.87 (s, 1H, H3), 5.64 (s, 1H, H7), 5.01 (t, J = 9.1 Hz, 1H, H4), 4.47 – 4.34 (m, 3H, H5 & H6 & H8), 4.25 (dd, J = 9.4, 6.2 Hz, 1H, H9"), 3.99 (dd, J = 9.4, 6.9 Hz, 1H, H9'), 3.81 (s, 3H, $COOCH_3$), 1.86 (s, 3H, CH_3), 1.35 (s, 3H, CH_3), 1.33 (s, 3H, CH_3). ^{13}C NMR (151 MHz, $CDCl_3$) δ 172.39 (C=O), 161.52 (C1), 158.82 (q, C=O), 156.82 (q, C=O), 145.32 (C2), 115.42 (m, CF_3), 114.75 (m, CF_3), 109.13 (C3), 108.76 ($(CH_3)_2C$-$(O)_2$), 77.37 (C6), 75.18 (C8), 72.35 (C7), 65.11 (C9), 52.76 (O-CH_3), 49.05 (C4), 45.92 (C5), 26.12 (CH_3), 25.34 (CH_3), 22.86 (CH_3). ^{19}F NMR (376 MHz, $CDCl_3$) δ -74.63 (s, 3F), -75.90 (s, 3F).

6.9 Methyl 5-acetamido-2,6-anhydro-4-[2,2,2-trifluoroacetamido]-3,4,5-trideoxy-8,9-*O*-(1-methylethylidene)-D-erythro-non-2-enonate (8ii)

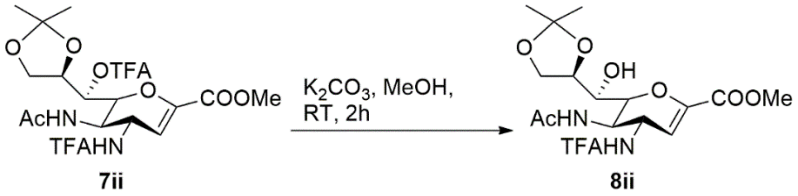

To a solution of **(6)** (0.0512 g, 0.138 mmol) in dry MeOH (5 ml) was added K_2CO_3 suspended in MeOH (2 ml). Upon completion (30 minutes, monitored by TLC) the reaction was quenched by adding a saturated NH_4Cl solution (10 ml) on ice. The aqueous layer was extracted with EtOAc (3 x 15 ml). The organic layers were combined, dried with Na_2SO_4, filtered and concentrated *in vacuo*. The crude was analysed without further purification. ^{1}H NMR (400 MHz, CD_3OD) δ 5.81 (d, J = 2.5 Hz, 1H, H3), 4.97 – 4.90 (m, 1H, H4), 4.32 (ddd, J = 7.5, 6.2, 5.4 Hz, 1H, H8), 4.27 – 4.18 (m, 2H, H5 & H6), 4.15 (dd, J = 8.7, 6.3 Hz, 1H, H9"), 4.01 (dd, J = 8.7, 5.5 Hz, 1H, H9'), 3.79 (s, 3H $COOCH_3$), 3.65 (d, J = 7.6 Hz, 1H, H7), 1.95 (s, 3H, CH_3), 1.38 (s, 3H, CH_3), 1.34 (s, 3H, CH_3). ^{13}C NMR (101 MHz, CD_3OD) δ 174.23 (C=O), 163.67 (C1), 146.65 (C2), 110.33 ($(CH_3)_2C$-$(O)_2$), 109.78 (C3), 76.25 (C8), 70.58 (C7), 67.87 (C9), 52.87 (O-CH_3), 27.17 (CH_3), 25.60 (CH_3), 22.58 (CH_3). ^{19}F NMR (376 MHz, CD_3OD) δ -77.38 (s, 3F).

6.10 Methyl 5-acetamido-2,6-anhydro-4-[(tert-butoxycarbonyl)amino]-7-(((methylsulfonyl)oxy)methyl)-3,4,5-trideoxy-8,9-*O*-(1-methylethylidene)-D-erythro-non-2-enonate (8i)

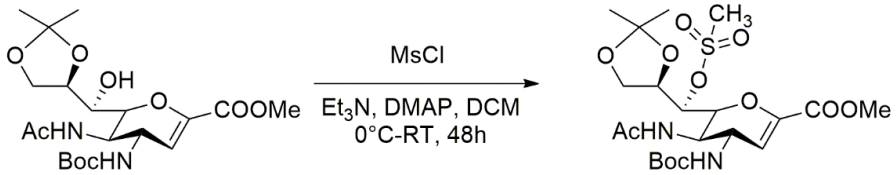

Compound **(7i)** (0.0261 g, 0.0587 mmol) was dissolved in dry DCM (5 ml) under nitrogen atmosphere. To this solution was added triethylamine (0.08 ml, 0.0529 mmol) and DMAP (0.0065g, 0.053 mmol) dissolved in 2 ml DCM, slowly on ice. Finally, on ice, methanesulfonyl chloride (0.018 ml, 0.235 mmol) was added dropwise and the reaction was left for 48h, slowly heating to RT. Upon completion (as indicated by TLC) the mixture was diluted with H_2O (15 ml) and EtOAc (10 ml). The aqueous layer was extracted with EtOAc (3 x 15 ml). The organic layers were combined, washed with 1M $KHSO_4$ (20 ml), saturated $NaHCO_3$ (20 ml), brine (25 ml), dried with Na_2SO_4, filtered, and concentrated in vacuo. The crude was further purified by column chromatography (EtOAc/PE, 8:2) to obtain (8i) as a white solid (0.022 g, 72% yield). ^{1}H NMR (400 MHz, $CDCl_3$) δ 6.20 (d, *J* = 8.5 Hz, 1H, NH), 5.91 (d, *J* = 2.0 Hz, 1H, C3), 5.14 (dd, *J* = 4.0, 1.7 Hz, 1H, C7), 4.84 (d, *J* = 8.1 Hz, 2H, C4), 4.75 (d, *J* = 10.2 Hz, 1H, C6), 4.38 (td, *J* = 6.7, 4.0 Hz, 1H, C8), 4.23 (dd, *J* = 9.1, 6.3 Hz, 1H, C9"), 4.05 (dd, *J* = 9.1, 7.2 Hz, 1H, C9'), 3.77 (s, 3H, $COOCH_3$), 3.68 (d, *J* = 9.0 Hz, 1H, H5), 3.19 (s, 3H, SO_2CH_3), 1.97 (s, 3H, CH_3), 1.43 (s, 4H, CH_3), 1.42 (s, 9H, CH_3), 1.34 (s, 3H, CH_3). ^{13}C NMR (101 MHz, $CDCl_3$) δ 161.96 (C=O), 155.86 (C=O), 111.36 (C3), 76.66 (C7), 76.16 (C6), 75.00 (C8), 65.54 (C9), 52.51 (O-CH_3), 49.77 (C5), 47.94 (C4), 39.12 (S-CH_3), 28.38 (3 x CH_3), 26.48 (CH_3), 25.12 (CH_3), 23.47 (CH_3).

6.11 2-Azidoethanol

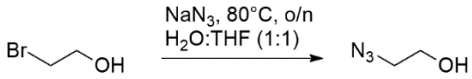

Sodium azide (0.7011 g, 10.784 mmol)) was dissolved in H_2O:THF (1:1, 20 ml). Next, 2-bromoethanol (0.5 ml, 7.054) was added dropwise over 5 minutes. The mixture was heated up to 50°C and reacted overnight. The mixture was extracted with diethyl ether (4 x 15 ml). The combined organic layers were dried with Na_2SO_4, filtered, and concentrated in vacuo. The crude was further purified by column chromatography (PE/diethyl ether, 7:3) to obtain 2-azidoethanol as a yellow liquid (0.153 g, 25% yield). ^{1}H NMR (400 MHz, $CDCl_3$) δ 3.83 – 3.74 (q, 2H), 3.49 – 3.42 (t, 2H).

6.12 3-Azidopropionic acid

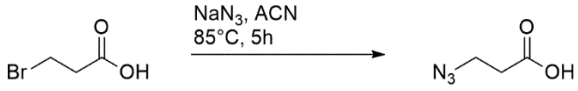

3-Bromopropionic acid (1.006 g, 6.580 mmol) was dissolved in acetonitrile (20 ml). Next, sodium azide (0.8713 g, 13.403 mmol) was while stirring. The mixture was left to react for 5 hours at 85°C. The mixture was concentrated under reduced pressure upon completion (as indicated by NMR). Next, the mixture was acidified using 1M HCl (pH = 5) and extracted with EtOAc (7 x 15 ml). The combined organic layers were dried with Na_2SO_4, filtered, and concentrated in vacuo. The crude 3-azidopropionic acid was used without further purification (0.465 g, 61% yield). ^{1}H NMR (400 MHz, $CDCl_3$) δ 3.60 (t, *J* = 6.5 Hz, 2H), 2.64 (t, *J* = 6.4 Hz, 2H). ^{13}C NMR (101 MHz, $CDCl_3$) δ 46.59 (CH_2), 33.67 (CH_2).

6.13 Methyl 5-acetamido-7,8,9-tri-*O*-acetyl-4-azido-3,4,5-trideoxy-3α-fluoro-D-erythro-*L*-glucononulopyranosonate (9eq) and Methyl 5-acetamido-7,8,9-tri-*O*-acetyl-4-azido-3,4,5-trideoxy-3β-fluoro-D-erythro-*L*-glucononulopyranosonate (9ax)

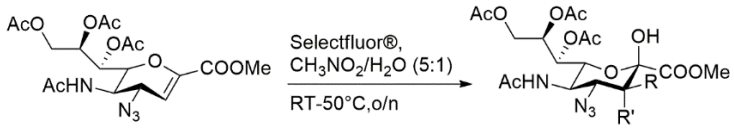

4

9eq: R = F, R' = H
9ax: R = H, R' = F

To a solution of compound **(4)** (1.000 g, 2.191 mmol) in nitromethane/H_2O (5:1, v/v, 20 ml) was added Selectfluor® (3.1118 g, 8.784 mmol). The suspension was left to react overnight at 50°C. When TLC revealed completion, the reaction was quenched with saturated NaHCO3 (40 ml). The aqueous layer was extracted with EtOAc (4 x 20 ml). The organic layers were combined, washed with saturated NaHCO3 (40 ml), brine (40 ml), dried with Na2SO4, filtered and concentrated in vacuo. The crude was further purified by column chromatography (DCM/EtOAc/acetone, 8:1:1-5:1:1) to obtain **(9eq)** (0.143 g, 13% yield) and **(9ax)** (0.406 g, 38% yield) as white solids. **(9ax)** ^{1}H NMR (400 MHz, acetone-d6) δ 7.30 (d, *J* = 7.9 Hz, 1H), 7.01 (s, 1H), 5.50 – 5.44 (m, 1H), 5.19 (ddd, *J* = 7.7, 4.5, 2.7 Hz, 1H), 5.04 (dd, 1H), 4.63 (dd, *J* = 12.2, 2.7 Hz, 1H), 4.45 (s, 2H), 4.15 (dd, *J* = 12.2, 7.7 Hz, 1H), 3.77 (s, 3H), 2.07 (s, 3H), 1.98 (s, 3H), 1.97 (s, 3H), 1.86 (s, 3H). ^{19}F NMR (376 MHz, acetone-d6) δ -204.16 (d, *J* = 40.6 Hz, C_3F-ax). **(9eq)** ^{1}H NMR (400 MHz, $CDCl_3$) δ 5.66 (d, *J* = 9.3 Hz, 1H), 5.29 (dd, *J* = 6.9, 2.0 Hz, 1H), 5.21 (ddd, *J* = 7.0, 6.3, 2.4 Hz, 1H), 4.82 – 4.62 (m, 2H), 4.39 (dd, *J* = 10.7, 2.1 Hz, 1H), 4.34 (dd, *J* = 12.5, 2.4 Hz, 1H), 4.23 (q, *J* = 10.6 Hz, 1H), 4.03 (dd, *J* = 12.5, 6.3 Hz, 1H), 3.94 (s, 3H), 3.71 (q, *J* = 10.3 Hz, 1H), 2.14 (s, 3H), 2.10 (s, 3H), 2.03 (s, 3H), 2.02 (s, 3H). ^{13}C NMR (101 MHz, $CDCl_3$) δ 170.81, 170.57, 170.38, 93.26 (d, *J* = 21.8 Hz), 90.14, 88.20, 70.08, 69.36, 67.61, 62.48, 54.48, 49.92, 23.52, 21.07, 20.94, 20.87. ^{19}F NMR (376 MHz, $CDCl_3$) δ -195.12 (dd, *J* = 48.9, 11.5 Hz, C_3F-eq).

6.14 Methyl 5-acetamido-7,8,9-tri-*O*-Acetyl-4-azido-3,4,5-trideoxy-2α,3β-difluoro-α-D-erythro-L-glucononulopyranosonate (10eq) and Methyl 5-acetamido-7,8,9-tri-*O*-Acetyl-4-azido-3,4,5-trideoxy-2α,3α-difluoro-α-D-erythro-L-glucononulo-pyranosonate (10ax)

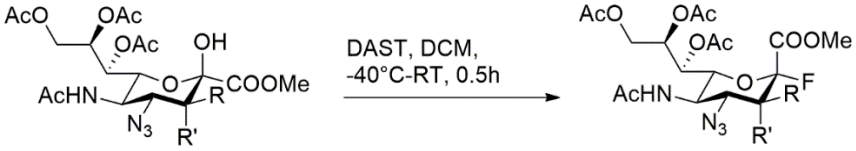

9eq: R = F, R' = H
9ax: R = H, R' = F

10eq: R = F, R' = H
10ax: R = H, R' = F

Compound **(9eq)** (0.406 g, 0.825 mmol) or **(9ax)** (0.222 g, 0.451 mmol) was dissolved in dry DCM under nitrogen atmosphere to form a suspension. Next, the mixture was cooled to -40°C and DAST (1.5 eq) was added dropwise. Upon completion (as indicated by TLC) the mixture was quenched with saturated $NaHCO_3$ solution (15 ml). The mixture was washed with brine (20 ml). The aqueous layer was extracted with DCM (3 x 15 ml). The organic layers were combined, washed with brine (25 ml), dried using Na_2SO_4, filtered and concentrated in vacuo. The crude was further purified by column chromatography (EtOAc/PE, 5:5-9:1) to obtain **(10eq)** (0.210 g, 94% yield) or **(10ax)** (0.315 g, 77% yield) as white solids. **(10ax)** ^{1}H NMR (400 MHz, $CDCl_3$) δ 5.90 (d, *J* = 7.3 Hz, 1H), 5.40 (ddd, *J* = 8.6, 4.4, 2.4 Hz, 1H), 5.26 (dt, *J* = 8.6, 1.6 Hz, 1H), 5.23 – 5.08 (m, 1H), 4.81 – 4.67 (m, 1H), 4.55 (d, *J* = 1.1 Hz, 1H), 4.36 (dd, *J* = 12.7, 2.4 Hz, 1H), 4.27 (dd, *J* = 12.7, 4.4 Hz, 1H), 3.91 (s, 3H), 3.33 (td, *J* = 10.8, 7.3 Hz, 1H), 2.18 (s, 3H), 2.12 (s, 3H), 2.05 (s, 5H). ^{13}C NMR (101 MHz, $CDCl_3$) δ 171.65, 171.53, 170.62, 169.83, 77.36, 70.62 (d, *J* = 4.4 Hz), 68.66, 67.69, 61.90, 53.97, 48.46 (d, *J* = 3.7 Hz), 23.75, 21.03, 20.95, 20.82. ^{19}F NMR (376 MHz, $CDCl_3$) δ -122.79 (d, *J* = 11.2 Hz, C_2F-eq), -216.97 (ddd, *J* = 50.1, 28.5, 11.3 Hz, C_3F-ax). **(10eq)** ^{1}H NMR (400 MHz, $CDCl_3$) δ 5.67 (d, *J* = 8.9 Hz, 1H), 5.31 (ddd, *J* = 8.0, 5.3, 2.6 Hz, 1H), 5.24 (dt, *J* = 8.4, 1.7 Hz, 1H), 4.69 (dd, *J* = 10.7, 1.6 Hz, 1H), 4.66 – 4.59 (m, 1H), 4.57 – 4.36 (m, 1H), 4.26 (dd, *J* = 12.5, 2.6 Hz, 1H), 4.16 – 4.10 (m, 1H), 3.91 (s, 3H), 3.64 (q, *J* = 10.3 Hz, 1H), 2.14 (s, 3H), 2.07 (s, 3H), 2.04 (s, 4H), 2.03 (s, 3H). ^{13}C NMR (101 MHz, $CDCl_3$) δ 170.70, 170.63, 170.60, 169.59, 77.36, 72.58, 68.75, 67.03, 62.14, 61.46, 53.65, 49.46 (d, *J* = 7.3 Hz), 23.53, 20.91, 20.90, 20.82. ^{19}F NMR (376 MHz, $CDCl_3$) δ -119.03 (t, *J* = 14.1 Hz, C_2F-eq), -197.16 (dt, *J* = 48.3, 13.6 Hz C_3F-eq).

6.15 5-Acetamido-3,4,5-trideoxy-4-azido-2α,3β-difluoro-α-D-erythro-L-glucononulo-pyranosonate (11eq) and 5-Acetamido-3,4,5-trideoxy-4-amino-2α,3α-difluoro-α-D-erythro-L-glucononulopyranosonate (11ax)

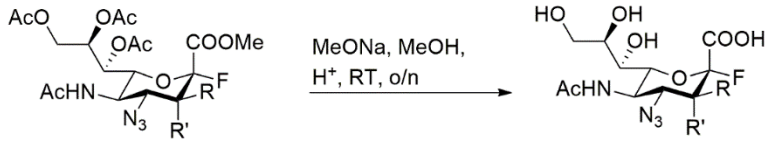

10eq: R = F, R' = H
10ax: R = H, R' = F

11eq: R = F, R' = H
11ax: R = H, R' = F

The starting material **(10ax)** (0.146 g, 0.295 mmol) was dissolved in dry MeOH (5 ml) and it was placed under nitrogen atmosphere. Next, a sodium methoxide (0.0125 g, 0.231 mmol) suspension in methanol (2 ml) was added to the mixture while on ice and heated up to RT. After 5 hours eight drops of 30% sodium methoxide solution in MeOH was added to the mixture dropwise, the observed pH was 11. The reaction was left at RT overnight. The mixture was neutralized with Amberlite IR-120 (H+) and the solvent was removed after filtration. The crude **(10ax)** (0.104, 99% yield) was used without further purification. ^{1}H NMR (400 MHz, CD_3OD) δ 5.33 – 5.16 (m, 1H), 4.45 (t, *J* = 10.9 Hz, 1H), 4.01 (qd, *J* = 9.7, 2.0 Hz, 2H), 3.85 – 3.76 (m, 2H), 3.69 – 3.60 (m, 1H), 3.57 (dt, *J* = 8.4, 1.7 Hz, 1H). ^{13}C NMR (101 MHz, CD_3OD) δ 174.49, 88.52 (dd, *J* = 189.4, 19.2 Hz), 75.12 (d, *J* = 3.7 Hz), 71.50, 69.45, 64.68, 61.19 (d, *J* = 22.5 Hz), 46.19 (d, *J* = 2.9 Hz), 22.71. ^{19}F NMR (376 MHz, CD_3OD) δ -124.45 (d, *J* = 10.7 Hz, C_2F-eq), -216.84 (ddd, *J* = 50.3, 29.1, 10.5 Hz, C_3F-ax).

6.16 Methyl 5-acetamido-3,4,5-trideoxy-4-azido-2α,3β-difluoro-α-D-erythro-L-glucononulo-pyranosonate (12eq) and Methyl 5-acetamido-3,4,5-trideoxy-4-amino-2α,3α-difluoro-α-D-erythro-L-glucononulopyranosonate (12ax)

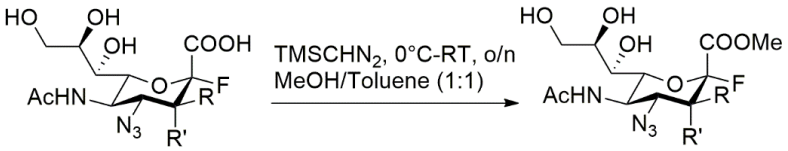

11eq: R = F, R' = H
11ax: R = H, R' = F

12eq: R = F, R' = H
12ax: R = H, R' = F

The starting material (11ax) (0.083 g, 0.234 mmol) was dissolved in MeOH/toluene (1:1, v/v, 6 ml) under nitrogen atmosphere. To the mixture was added $TMSCHN_2$ (0.3 ml, 0.586 mmol, 2M solution in hexanes) dropwise at 0°C and stirred overnight. The solvent was removed under reduced pressure upon completion (as indicated by TLC). The crude was further purified by column chromatography (DCM/MeOH, 98:2-90:10) to obtain (12ax) (0.063 g, 73% yield) as a white solid. ^{1}H NMR (400 MHz, CD_3OD) δ 5.26 (dt, 1H), 4.45 (t, *J* = 10.9 Hz, 1H), 4.12 – 3.95 (m, 2H), 3.89 (s, 3H), 3.81 – 3.73 (m, 2H), 3.68 – 3.62 (m, 1H), 3.55 (ddd, *J* = 9.3, 2.2, 1.3 Hz, 1H), 2.01 (s, 3H). ^{19}F NMR (376 MHz, CD_3OD) δ -124.88 (d, *J* = 10.4 Hz, C_2F-eq), -217.02 (ddd, *J* = 50.1, 29.2, 10.5 Hz, C_3F-ax).

7 Acknowledgements

First of all, I would like to thank Tom Wennekes for providing me with the opportunity to do an internship in the WennekesLab. His expertise in organic chemistry helped me tremendously throughout my internship. Secondly, I would like to thank Lemeng Chao for her daily supervision. Her vast knowledge and experience in the organic chemistry laboratory were incredibly helpful and I learned a lot from her throughout my internship. Finally, I would like to thank all the people in the east-laboratory on the fifth floor in the David de Wied building for creating a nice environment and always helping me whenever I had questions or issues.

8 References

1. Wang, B. and J. Brand-Miller, *The role and potential of sialic acid in human nutrition.* European Journal of Clinical Nutrition, 2003. **57**(11): p. 1351-1369.

2. Ghosh, S., *Chapter 1 - Sialic acid and biology of life: An introduction*, in *Sialic Acids and Sialoglycoconjugates in the Biology of Life, Health and Disease*, S. Ghosh, Editor. 2020, Academic Press. p. 1-61.

3. Chen, X. and A. Varki, *Advances in the Biology and Chemistry of Sialic Acids.* Acs Chemical Biology, 2010. **5**(2): p. 163-176.

4. Liu, G.J., L.Y. Jia, and G.W. Xing, *Probing Sialidases or Siglecs with Sialic Acid Analogues, Clusters and Precursors.* Asian Journal of Organic Chemistry, 2020. **9**(1): p. 42-52.

5. Iuliano, A.D., K.M. Roguski, and H.H. Chang, *Estimates of global seasonal influenza-associated respiratory mortality: a modelling study (vol 391, pg 1285, 2018).* Lancet, 2018. **391**(10127): p. 1262-1262.

6. Lampejo, T., *Influenza and antiviral resistance: an overview.* European Journal of Clinical Microbiology & Infectious Diseases, 2020. **39**(7): p. 1201-1208.

7. Yuan, L., Y. Zhao, and X.L. Sun, *Sialidase substrates for Sialdiase assays-activity, specificity, quantification and inhibition.* Glycoconjugate Journal, 2020. **37**(5): p. 513-531.

8. Kim, J.H., et al., *Mechanism-based covalent neuraminidase inhibitors with broad-spectrum influenza antiviral activity.* Science, 2013. **340**(6128): p. 71-5.

9. Wei, F., et al., *Regioselective synthesis of multisubstituted 1,2,3-triazoles: moving beyond the copper-catalyzed azide-alkyne cycloaddition.* Chemical Communications, 2016. **52**(99): p. 14188-14199.

10. Tsai, C.S., et al., *Cell-permeable probe for identification and imaging of sialidases.* Proc Natl Acad Sci U S A, 2013. **110**(7): p. 2466-71.

11. Malapelle, A., et al., *An expeditious synthesis of N-acetylneuraminic acid alpha-C-glycosyl derivatives ("alpha-C-glycosides") from the anomeric acetates.* European Journal of Organic Chemistry, 2007. **2007**(19): p. 3145-3157.

12. Shidmoossavee, F.S., J.N. Watson, and A.J. Bennet, *Chemical Insight into the Emergence of Influenza Virus Strains That Are Resistant to Relenza.* Journal of the American Chemical Society, 2013. **135**(36): p. 13254-13257.

13. Bennet, A. and I. Hemeon, *Sialic Acid and Structural Analogues: Stereoselective Syntheses.* Synthesis, 2007. **2007**(13): p. 1899-1926.

14. Dinh, H., et al., *Glycan based Detection and Drug Susceptibility of Influenza Virus.* Analytical Chemistry, 2014. **86**(16): p. 8238-8244.

15. Yang, Z.L., et al., *Synthesis of multivalent difluorinated zanamivir analogs as potent antiviral inhibitors.* Tetrahedron Letters, 2016. **57**(24): p. 2579-2582.

16. Liu, K.C., et al., *Enhanced Anti-influenza Agents Conjugated with Anti-inflammatory Activity.* Journal of Medicinal Chemistry, 2012. **55**(19): p. 8493-8501.

17. Lu, Y. and J. Gervay-Hague, *Synthesis of C-4 and C-7 triazole analogs of zanamivir as multivalent sialic acid containing scaffolds.* Carbohydrate Research, 2007. **342**(12-13): p. 1636-1650.

18. Fraser, B.H., et al., *Synthesis of 1,4-triazole linked zanamivir dimers as highly potent inhibitors of influenza A and B.* Medchemcomm, 2013. **4**(2): p. 383-386.

19. Nyffeler, P.T., et al., *Selectfluor: mechanistic insight and applications.* Angew Chem Int Ed Engl, 2004. **44**(2): p. 192-212.

20. Andrews, D.M., et al., *Synthesis and influenza virus sialidase inhibitory activity of analogues of 4-Guanidino-Neu5Ac2en (Zanamivir) modified in the glycerol side-chain.* European Journal of Medicinal Chemistry, 1999. **34**(7-8): p. 563-574.

21. Khedri, Z., et al., *Chemoenzymatic synthesis of sialosides containing C7-modified sialic acids and their application in sialidase substrate specificity studies.* Carbohydrate Research, 2014. **389**: p. 100-111.

22. Ying, J., Q. Gao, and X.F. Wu, *Zinc-catalyzed transformation of diarylphosphoryl azides to diarylphosphate esters and amides.* Chem Asian J, 2020. **15**(10): p. 1540-1543.

23. Hein, J.E., A. Armstrong, and D.G. Blackmond, *Kinetic profiling of prolinate-catalyzed alpha-amination of aldehydes.* Org Lett, 2011. **13**(16): p. 4300-3.

24. Redwan, I.N. and M. Grøtli, *Method for Activation and Recycling of Trityl Resins.* The Journal of Organic Chemistry, 2012. **77**(16): p. 7071-7075.

25. Chanteau, S.H. and J.M. Tour, *Synthesis of Anthropomorphic Molecules: The NanoPutians.* The Journal of Organic Chemistry, 2003. **68**(23): p. 8750-8766.

26. *Ethyl Isocyanate*. 1999, National Institute of Advanced Industrial Science and Technology (AIST) Japan.

9 Supplementary information

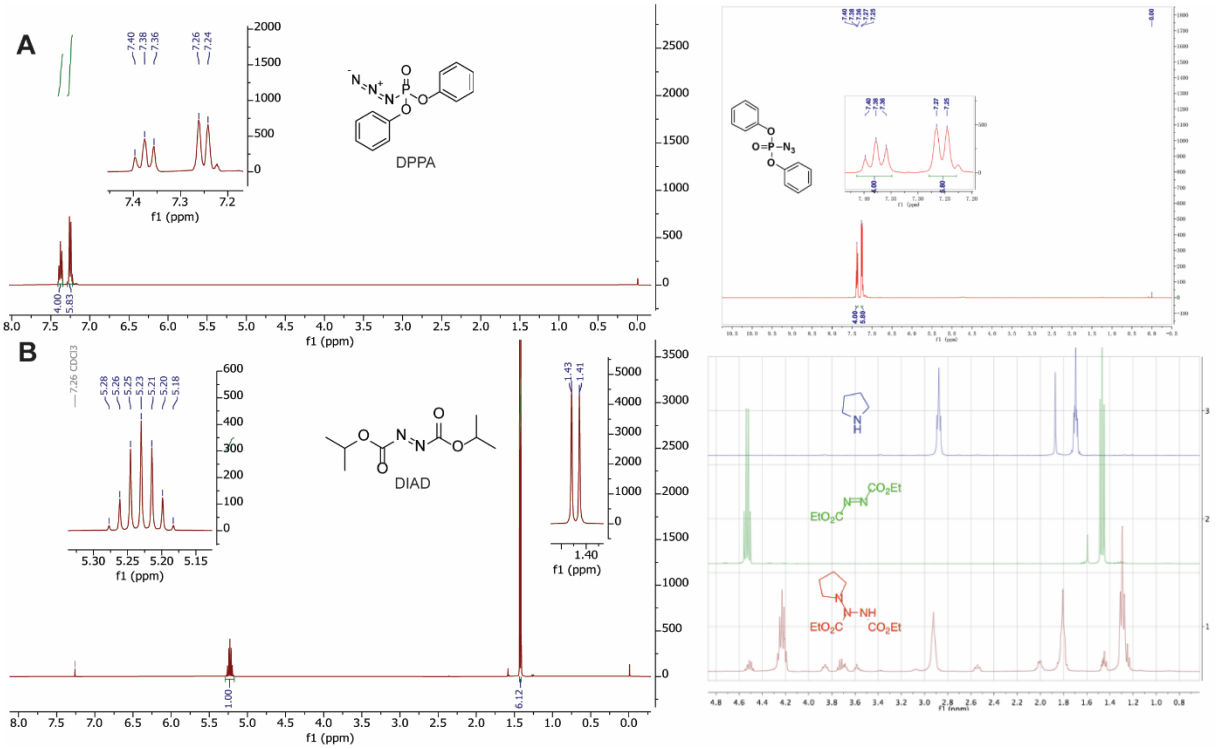

Figure S1 A) Measured [1]HNMR spectrum of diphenylphosphoryl azide (DPPA), with a zoom in on the aromatic peaks (left), compared to a literature reference [1]HNMR spectrum of DPPA (right) [22]. B) Measured [1]HNMR spectrum of diisopropyl azodicarboxylate (DIAD), with a zoom in on the aromatic and alkane peaks (left), compared to a literature reference [1]HNMR spectrum of DIAD (middle spectrum, right) [23].

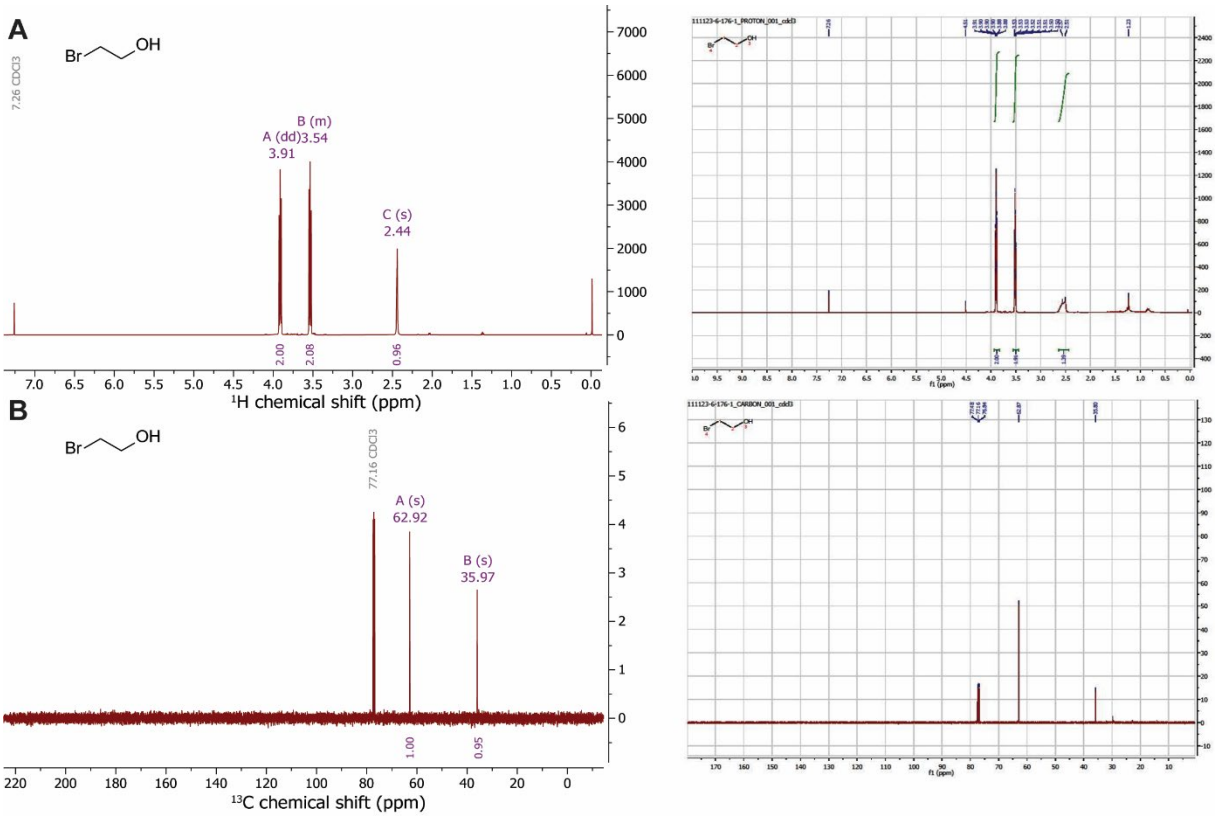

Figure S2 A) Measured [1]HNMR spectrum of 2-bromoethanol (left), compared to a literature reference [1]HNMR spectrum of 2-bromoethanol (right) [24]. B) Measured [13]CNMR spectrum of 2-bromoethanol (left), compared to [13]CNMR spectrum of 2-bromoethanol (right) [24].

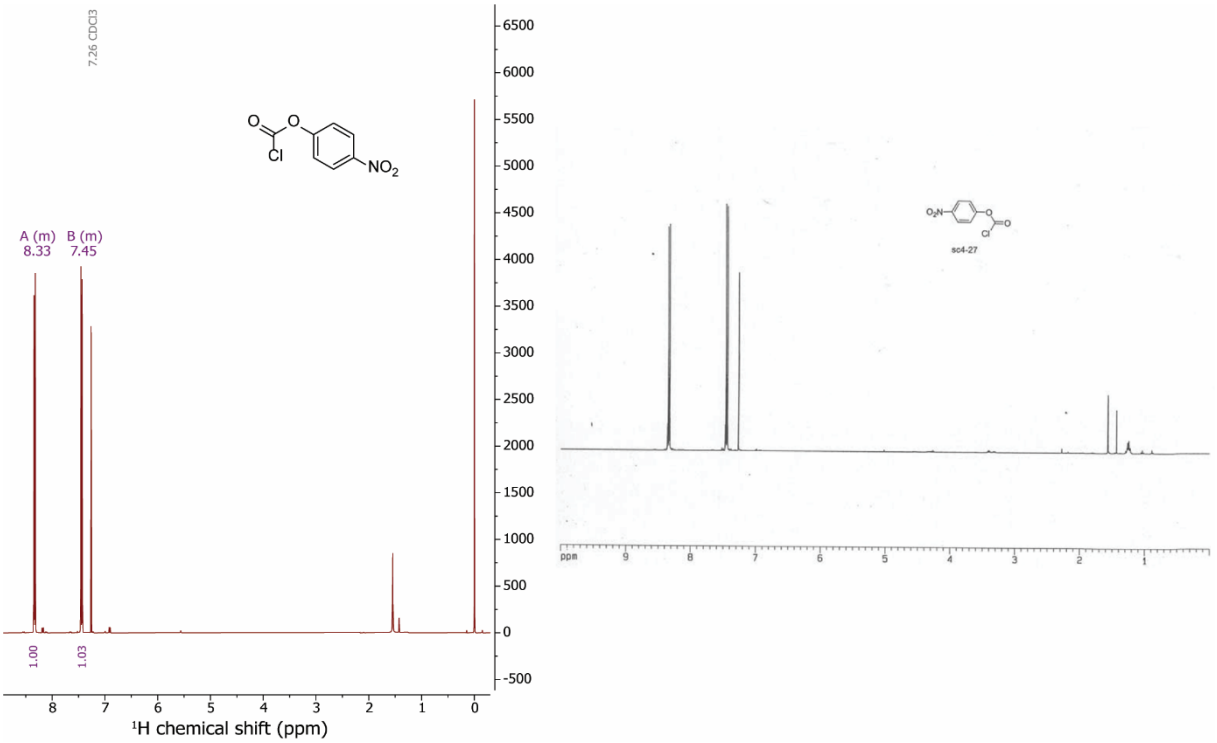

Figure S3 Measured [1]HNMR spectrum of 4-nitrophenyl chloroformate (left), compared to a literature reference [1]HNMR spectrum of 4-nitrophenyl chloroformate (right) [25].

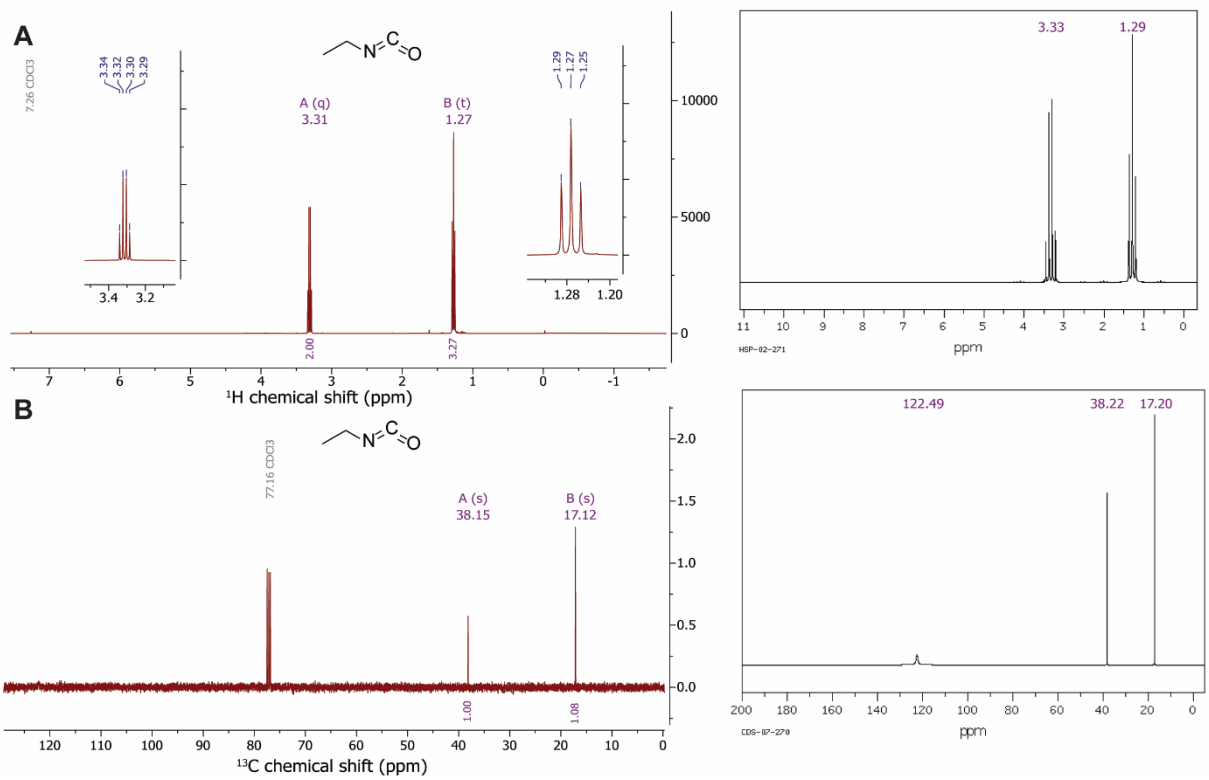

Figure S4 A) Measured ^{1}HNMR spectrum of ethyl isocyanate, with a zoom in on the peaks to visualize the splitting (left), compared to a literature reference ^{1}HNMR spectrum of ethyl isocyanate (right) [26]. B) Measured ^{13}CNMR spectrum of ethyl isocyanate (left), compared to a literature reference ^{13}CNMR spectrum of ethyl isocyanate (right) [26].